https://doi.org/10.5194/egusphere-2026-3722
Preprint. Discussion started: 27 July 2026

Trophic amplification of Southern Ocean plankton emerges from changing seasonality

Tianfei Xue[1], Lionel A. Arteaga[2,3], Markus Pahlow[1], and Ivy Frenger[1]

[1]GEOMAR Helmholtz Centre for Ocean Research Kiel, Kiel, 24148, Germany
[2]Global Modeling and Assimilation Office, NASA Goddard Space Flight Center, Greenbelt, MD 20771, USA
[3]Goddard Earth Sciences, Technology and Research II, University of Maryland, Baltimore County, Baltimore, MD 21250, USA

Correspondence: Tianfei Xue (txue@geomar.de)

Abstract. Understanding how climate change will alter plankton dynamics in the Southern Ocean, a region of globally significant biogeochemical influence and strong seasonal variability, is critical for projecting the future of ocean ecosystems. Using a multi-model ensemble of 12 earth system models under the SSP5-8.5 climate-change scenario, we show that the seemingly stable Southern Ocean-wide plankton biomass masks opposing trends across three distinct biogeochemical zones. Plankton in the subpolar zone (40°S–60°S) remains near-stable owing to compensatory changes in bottom-up and top-down processes. In the subtropical zone (30°S–40°S) and seasonal ice zone (60°S–90°S), zooplankton decline and increase proportionally more than phytoplankton, constituting negative and positive trophic amplification, respectively. This trophic amplification is not uniformly distributed throughout the year but arises primarily from austral spring and summer. In the subtropical zone, shoaling-induced nutrient limitation reduces phytoplankton growth and concentration, causing a disproportionate decline in zooplankton grazing and biomass. In the seasonal ice zone, improved light availability from mixed-layer shoaling, sea-ice retreat, and warming enhance phytoplankton growth and surface concentration, driving disproportionately enhanced zooplankton grazing and biomass. In both zones, the seasonal trophic amplification signal is substantially stronger during the ecologically important spring and summer seasons than over the annual-mean, with potentially severe ecological consequences. Our results demonstrate that annual-mean projections could systematically underestimate both the magnitude and ecological severity of trophic amplification, and highlight the need for assessing seasonal and regional variations in plankton dynamics to better constrain future projections of Southern Ocean ecosystems.

1 Introduction

Understanding how climate change will restructure trophic interactions at the base of the marine food web is fundamental to projecting the ecological future of the ocean. Changes in plankton productivity and biomass, as well as alterations in population dynamics, can trigger cascading effects throughout marine food webs. The dynamics of plankton are governed by the interplay of bottom-up (e.g., nutrient supply and light availability) and top-down (e.g., predation) processes, which respond to changes in environmental conditions susceptible to climate change (Marinov et al., 2010; Stock et al., 2014). Existing studies suggest trophic amplification in response to reduced marine phytoplankton biomass and productivity in a warmer climate, leading to

https://doi.org/10.5194/egusphere-2026-3722
Preprint. Discussion started: 27 July 2026

more pronounced declines at higher trophic levels (Chust et al., 2014; Kwiatkowski et al., 2019; Lotze et al., 2019). Previous studies on future changes in plankton due to climate change have predominantly focused on long-term shifts in mean-state properties (Sarmiento et al., 2004b; Steinacher et al., 2010; Kwiatkowski et al., 2020; Xue et al., 2024b), rather than seasonality.

Seasonality plays an important role in coupling phytoplankton dynamics to higher trophic levels (Xue and Hill, 2025). Different trophic levels are governed by different seasonal drivers, with phytoplankton responding to more light and nutrient availability (Doney, 2006) and fish more to temperature and food availability (Asch et al., 2019), and are therefore likely to respond differently to climate change not only in terms of long-term trends (Chust et al., 2014; Stock et al., 2014), but also on a seasonal time scale (Yamaguchi et al., 2022; Xue and Hill, 2025). Evidence for such differential seasonal responses is already emerging: Climate-change-induced phenological shifts in phytoplankton could exceed natural background variability by the end of the century (Yamaguchi et al., 2022), while higher trophic levels such as fish have already shown seasonal shifts in response to global warming over recent decades (Edwards and Richardson, 2004). Whether and how these differential responses lead to seasonal trophic amplification under climate change, and what the driving mechanisms could be, remains unresolved.

Plankton in the Southern Ocean, a region of strong seasonal fluctuations (Thomalla et al., 2011; Deppeler and Davidson, 2017; Arteaga et al., 2020), plays a crucial role not only in the local food web but also in shaping the biogeochemical characteristics of the global ocean (Sarmiento et al., 2004a; Le Quéré et al., 2016; Nissen et al., 2021). Climate change is likely to alter plankton dynamics throughout the Southern Ocean, with specific changes expected to vary among regions (Leung et al., 2015; Deppeler and Davidson, 2017). Using state-of-the-art climate model projections across three distinct biogeochemical zones, we demonstrate that trophic amplification in the Southern Ocean is fundamentally a seasonal phenomenon whose intensity substantially exceeds that of the annual-mean signal, and that its magnitude and sign differ markedly across zones. Our results highlight the importance of accounting for distinct biogeochemical zones (Fig. 1) and seasonal variations when addressing the ecological future of the Southern Ocean as a whole.

2 Method

2.1 Multi-Model Ensemble

We use the output of a Multi-Model Ensemble (MME; Table 1) of 12 Earth System Models (ESMs) to diagnose future plankton changes in the Southern Ocean. Ten of these ESMs are part of the Coupled Model Intercomparison Project Phase 6 (CMIP6, downloaded from https://esgf-data.dkrz.de). The Flexible Ocean and Climate Infrastructure version 1 (FOCI) model (Chien et al., 2022) and the Optimality-based non-Redfield plankton-ecosystem model (OPEM v1.1) in UVic-ESCM 2.9 (Pahlow et al., 2020) were added to these 10 models. The selection of these models is based on the availability of the archived variables required for our analysis (mixed layer depth, phytoplankton and zooplankton biomass concentrations), the temporal resolution (monthly), and the experimental settings (historical simulation, preindustrial control simulation to account for potential drifts, and the SSP5-8.5 high-emission-no-mitigation scenario). The models within the MME are structurally different, cover a range of different parameterizations of processes, and use different initial conditions (Séférian et al., 2020). Notably, the UVic-OPEM

https://doi.org/10.5194/egusphere-2026-3722
Preprint. Discussion started: 27 July 2026

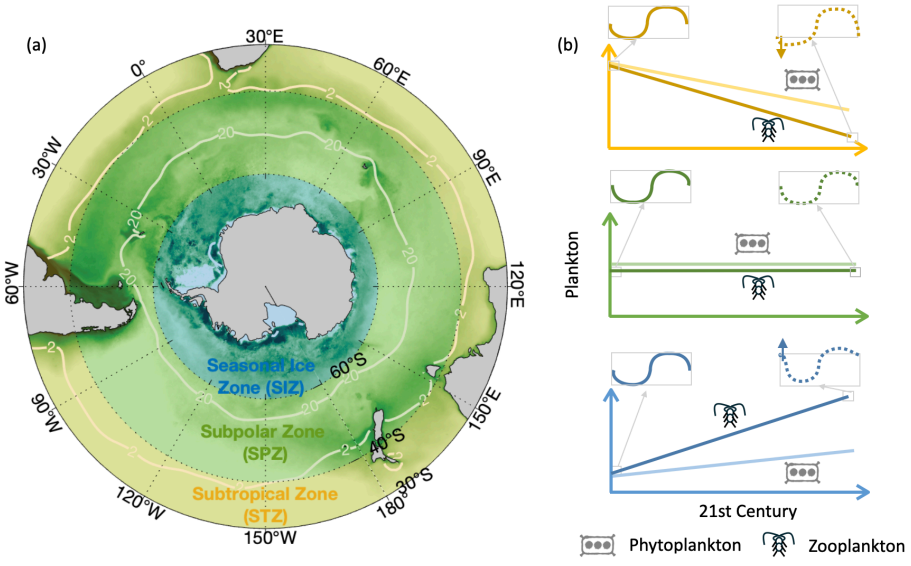

Figure 1. (a) Illustration of research areas in the Southern Ocean: Subtropical Zone (STZ: 30°S - 40°S, yellow), Subpolar Zone (SPZ: 40°S - 60°S, green), and Seasonal Ice Zone (SIZ: 60°S - 90°S, blue), overlaid on a map of climatolgical surface chlorophyll (green shading, from MODIS, with darker shading indicating higher concentrations) and surface nitrate concentrations (in mmol m^{-3}, white contours, from the World Ocean Atlas: https://www.ncei.noaa.gov/products/world-ocean-atlas). (b) Simplified schematic of projections from a multi-model ensemble for the 21st century summarized schematically. The STZ shows negative trophic amplification, where zooplankton decline more than phytoplankton in response to climate change, mostly during austral spring and summer (downward arrow). No significant changes in plankton and its seasonality are expected in the SPZ. The SIZ shows positive trophic amplification, also mostly during austral spring and summer (upward arrow).

model uses an optimality-based framework for nutrient uptake and growth (Pahlow et al., 2020), in contrast to the fixed-stoichiometry or empirical parameterizations used in most CMIP6 models, providing an independent constraint on projected responses. All output fields were regridded onto a regular $1° \times 1°$ grid using the bilinear interpolation of Climate Data Operators (CDO). The output of the MME has been validated against observations (Section 2.3 and Appendix A). While individual models exhibit substantial differences in absolute values, particularly for biological variables (Xue et al., 2024b; Le Grix and Tagliabue, 2026), they show strong agreement in the projected relative changes. This consistency suggests agreement on systemic trends and supports the use of MMEs for assessing future plankton dynamics.

2.2 Geographic Zones

The Southern Ocean exhibits, to first order, a zonally banded pattern in terms of its biogeochemical properties. Based on the observed patterns of surface nutrient and chlorophyll concentrations and previous findings on the mechanisms driving

https://doi.org/10.5194/egusphere-2026-3722
Preprint. Discussion started: 27 July 2026

Table 1. Multi-Model Ensemble (MME) Overview for Study

No.	Model Name	Ocean Biogeochemistry	Plankton Groups[$]	Reference
(a)	CanESM5	CMOC	P1Z1	Swart et al. (2019)
(b)	CanESM5-CanOE[†]	CanOE*	P2Z2	Christian et al. (2022)
(c)	CESM2-WACCM [‡]	MARBL*	P3Z1	Danabasoglu et al. (2020)
(d)	CNRM-ESM2-1[†]	PISCESv2-gas*	P2Z2	Séférian et al. (2019)
(e)	FOCI1[†]	MOPS	P1Z1	Chien et al. (2022)
(f)	GFDL-ESM4[†]	COBALTv2*	P3Z3	Dunne et al. (2020)
(g)	IPSL-CM6A-LR [‡]	PISCES-v2*	P2Z2	Boucher et al. (2020)
(h)	MPI-ESM1.2-HR[†] [‡]	HAMOCC6*	P2Z1	Müller et al. (2018)
(i)	MRI-ESM2.0 [‡]	NPZD	P1Z1	Tsujino et al. (2017)
(j)	NorESM2-MM	iHAMOCC*	P2Z1	Tjiputra et al. (2020)
(k)	UKESM1-0-LL[†]	MEDUSA *	P2Z2	Sellar et al. (2019)
(l)	UVic-OPEM[†]	OPEM *	P2Z1	Pahlow et al. (2020)

[†] includes both phytoplankton production and zooplankton grazing in output

[‡] includes sea ice extent in output

* explicitly includes iron limitation

[$] PxZy indicates x phytoplankton and y zooplankton groups

phytoplankton seasonality under current climate conditions (Arteaga et al., 2020; Thomalla et al., 2023b), we have divided the Southern Ocean into three distinct latitudinal zones (Fig. 1):

- The **Subtropical Zone (STZ)** spans the latitudinal range between 30°S and 40°S (Fig. 1, yellow), representing oligotrophic waters with low surface nitrate and chlorophyll concentrations. Observations indicate a relatively shallow mean mixed-layer depth (MLD) and the lowest phytoplankton and low zooplankton biomass among the three zones (Fig. 2a,d,g and Table 2).

- The **Subpolar Zone (SPZ)** covers the zonal band between 40°S and 60°S (Fig. 1, green), characterized by abundant surface nitrate. The seasonality of phytoplankton is driven by a variety of bottom-up (light and iron limitation) and top-down (zooplankton grazing) processes (Boyd et al., 2001; Hiscock et al., 2003; Deppeler and Davidson, 2017). Observations indicate the deepest MLD, relatively high phytoplankton and variable zooplankton biomass (Fig. 2b,e,h and Table 2).

- The **Seasonal Ice Zone (SIZ)** is the area south of 60°S (Fig. 1, blue), heavily influenced by seasonally varying light and sea ice conditions. Changes in sea ice concentration, extent, and seasonality play a crucial role in determining light availability and thereby the timing and extent of phytoplankton blooms (Deppeler and Davidson, 2017; Westwood et al., 2010). Observations indicate intermediate MLD, a strongly seasonal yet relatively low phytoplankton biomass, partly due to the shortened growth season, and high zooplankton biomass (Fig. 2c,f,i and Table 2).

https://doi.org/10.5194/egusphere-2026-3722
Preprint. Discussion started: 27 July 2026

Table 2. Definitions and average characteristics of the research areas (zones).

Zone	Mixed Layer Depth (m)			Phytoplankton (mmol C m^{-2})		Zooplankton (mmol C m^{-2})		
	Argo	BGC-Argo	MME	BGC-Argo	MME	Yang 2022	COPEPOD	MME
STZ (30–40°S)	63.7 ± 0.2	67.0 ± 3.3	60.1 ± 3.6	48.1 ± 2.8	158.5 ± 22.1	19.0 ± 2.4	38.2 ± 7.4	116.0 ± 24.5
SPZ (40–60°S)	112.9 ± 0.2	100.0 ± 3.7	99.7 ± 6.0	75.7 ± 2.4	169.9 ± 30.0	52.2 ± 3.6	38.2 ± 5.4	115.3 ± 27.7
SIZ (60–90°S)	100.6 ± 0.3	65.2 ± 3.6	93.5 ± 6.9	53.1 ± 3.9	96.1 ± 25.9	40.2 ± 3.5	48.9 ± 7.4	55.6 ± 24.5

$\pm$ values indicate one standard error of the mean, representing inter-model spread for the MME and spatial variability across in situ sampling locations for observational datasets.

2.3 Model validation

2.3.1 Mixed layer depth

Simulated mixed-layer depth (MLD) under the current climate, is validated against observed MLD estimates for 2010–2024 derived from BGC-Argo data (Fig. A1, https://argo.ucsd.edu/data/data-from-gdacs/) and against the Argo mixed-layer product for 2000–2021 (https://mixedlayer.ucsd.edu/, Holte et al., 2017). Estimates of MLD from the BGC-Argo float data (Frenzel et al., 2022, section A) are derived from temperature and density measurements following the methodology of de Boyer Montégut et al. (2004). Overall, the simulated MLD fields in the individual models capture the observed climatological spatial pattern, with the SPZ generally exhibiting deeper MLD than the rest of the Southern Ocean (Table 2). However, some models simulate an especially deep MLD region close to the coast, particularly in the Weddell Sea (Fig. A2), possibly owing to deep convection events. This feature is much less pronounced in both observational products. In addition to reproducing the climatological mean spatial pattern, the regional mean MLD in the STZ and SPZ generally agree with both observational products. In the SIZ, the modelled MLD is close to that of the Argo product, but both are substantially deeper than the BGC-Argo estimate (Table 2), which may reflect the relatively sparse coastal coverage of BGC-Argo (Fig. A2). Despite a lag of 1 to 3 weeks in the STZ, SPZ, and SIZ (Fig. 2a–c), the MME reasonably captures the relative amplitude of MLD seasonality (Fig. 2). This is particularly relevant to our study, given the crucial role of the dilution effect in shaping light availability for phytoplankton growth (Xue et al., 2022b), in distributing the phytoplankton over the water column, and ultimately in zooplankton grazing (Xue et al., 2022a).

2.3.2 Integrated phytoplankton carbon

Observational estimates of vertically integrated phytoplankton carbon follow the method used in Arteaga et al. (2020). Argo-float bbp(700) data serve as the basis for estimating particulate organic carbon (POC, mg m^{-3}, Eq. 1), which is subsequently used to estimate phytoplankton carbon (C_{phy}, mg m^{-3}, Eq. 2; Haëntjens et al., 2017; Graff et al., 2015):

$$\mathrm{POC} = 3.12 \times 10^4 (\pm 2.47 \times 10^3) \times \mathrm{bbp}(700) + 3.0(\pm 6.8) \quad (1)$$

https://doi.org/10.5194/egusphere-2026-3722
Preprint. Discussion started: 27 July 2026

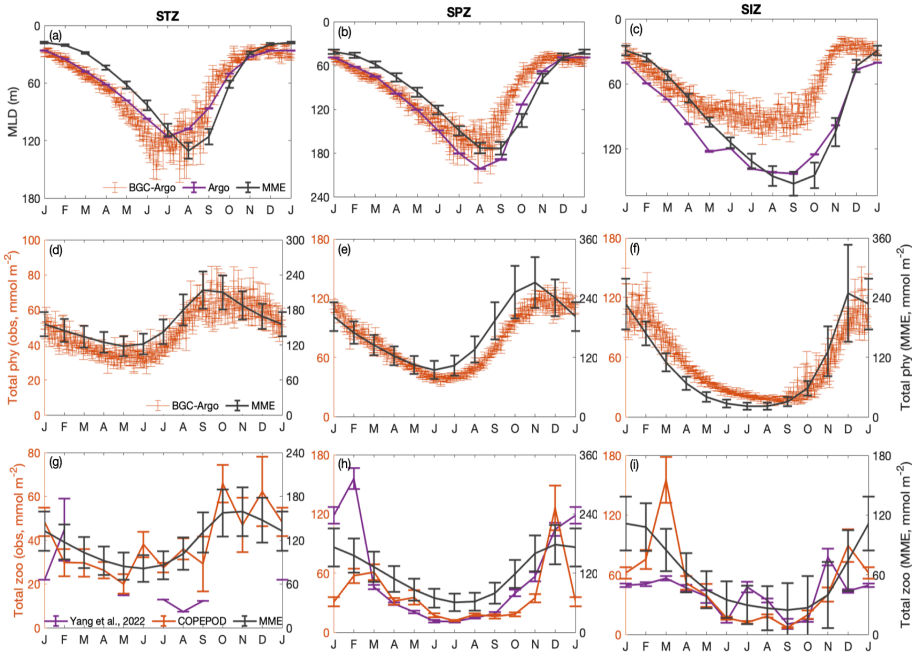

Figure 2. Annual cycles of mixed layer depth (MLD, in m), total phytoplankton and zooplankton biomass (in mmol C m^{-2}) in the subtropical zone (STZ), subpolar zone (SPZ), and seasonal ice zone (SIZ). (a–c) MLD, (d–f) phytoplankton biomass integrated over the entire water column, and (g–i) integrated zooplankton biomass from observational data (left axis) and MME (right axis). Black lines represent the mean values from the MME. Red lines indicate daily BGC-Argo estimates for MLD and phytoplankton biomass (panels a–f), and monthly zooplankton biomass from the COPEPOD dataset (O'Brien, 2007) (panels g–i). Purple lines show monthly MLD from the Argo mixed-layer product (Holte et al., 2017) in panels (a–c), and monthly zooplankton biomass from Yang et al. (2022) (panels g–i). Error bars represent the standard error of the mean for both the MME (inter-model uncertainty) and the observational datasets (spatial patchiness of in situ data).

105

$$C_{phy} = 0.19 \times POC \pm 8.7 \quad (2)$$

Similar to MLD, the modelled seasonal variation in integrated phytoplankton carbon is validated against BGC-Argo estimates, as shown in Fig. 2d–f. Modelled phytoplankton biomass is substantially higher than the observational estimates in the STZ and SPZ. Across all three zones, observed phytoplankton biomass is at a similar level to zooplankton biomass (Sect. 2.3.3),
110 indicating a "top-heavy" system, as also noted by Yang et al. (2022). This may result from substantial zooplankton omnivory (McCauley et al., 2018) or from higher phytoplankton than zooplankton turnover rates (Shurin et al., 2006). These distinctive "top-heavy" features reflect complex ecological and biogeochemical dynamics that current climate models are not yet able to capture fully. Moreover, the modelled phytoplankton seasonal cycles in the three geographical zones appear up to 1 month earlier than the observed float-based estimates (Fig. 2d–f). This is likely because most models are calibrated with satellite
115 chlorophyll data rather than in situ carbon biomass measurements, and chlorophyll typically peaks before carbon biomass

https://doi.org/10.5194/egusphere-2026-3722
Preprint. Discussion started: 27 July 2026

(Vives et al., 2024). Nevertheless, the MME reproduces the amplitude of seasonal variation reasonably well, providing a basis for projecting seasonally uneven responses of plankton communities to future climate change.

2.3.3 Integrated zooplankton carbon

Modelled integrated zooplankton biomass is validated against monthly integrated mesozooplankton biomass from two observational datasets: the COPEPOD database (O'Brien, 2007) and the dataset compiled by Yang et al. (2022), which includes observations spanning from 1932 to 2020 (Fig. 2g–i). In the STZ and austral winter in SPZ, the modelled zooplankton biomass is substantially higher than the measured biomass in the COPEPOD dataset and in situ data in Yang et al. (2022), which could be the result of an overestimated phytoplankton biomass. Yet, the MME broadly reproduces the observed seasonal patterns, including the timing and magnitude of seasonal peaks and troughs. The MME captures the seasonal variation of zooplankton biomass under the current climate reasonably well in the SIZ (Fig. 2i).

2.4 Analysis of phenological changes

Following the approach used in previous phenological analyses (Behrenfeld et al., 2017; Yamaguchi et al., 2022), we focus on the total plankton biomass. To investigate the mechanistic drivers of phytoplankton phenological changes, we examine the two main contributors of phytoplankton biomass (phy) change, namely the seasonal variations in phytoplankton growth rate (μ, in d^{-1}, Eq. 3) and mortality rate owing to zooplankton grazing (g, in d^{-1}, Eq. 4), based on primary production (PP, in $\mathrm{mmol\,C\,m^{-2}d^{-1}}$), zooplankton grazing flux ($GRAZ$, in $\mathrm{mmol\,C\,m^{-2}d^{-1}}$), using monthly data.

$$\mu = \frac{PP}{\mathrm{phy}} \tag{3}$$

$$g = \frac{GRAZ}{\mathrm{phy}} \tag{4}$$

Further, we evaluate monthly rates of change (tendencies) in total biomass by analyzing the budgets of integrated phytoplankton (phy, in $\mathrm{mmol\,C\,m^{-2}}$, Eq. 5) and zooplankton biomass (zoo, in $\mathrm{mmol\,C\,m^{-2}}$, Eq. 6) over the entire water column. We then assess how their tendencies (T_{phy} and T_{zoo}, in $\mathrm{mmol\,C\,m^{-2}d^{-1}}$) are governed by a dynamically balanced budget that includes primary production (PP), zooplankton grazing ($GRAZ$), and other processes (O):

$$T_{\mathrm{phy}} = \frac{\mathrm{d\,phy}}{\mathrm{d}t} = PP - GRAZ - O_{\mathrm{phy}} \tag{5}$$

$$T_{\mathrm{zoo}} = \frac{\mathrm{d\,zoo}}{\mathrm{d}t} = GRAZ - O_{\mathrm{zoo}} \tag{6}$$

where $\mathrm{d\,phy}/\mathrm{d}t$ and $\mathrm{d\,zoo}/\mathrm{d}t$ are calculated offline as the rates of change in phytoplankton and zooplankton biomass, and PP and $GRAZ$ are obtained directly from the model outputs listed in Table 1 (denoted by †). Because absolute values, especially

https://doi.org/10.5194/egusphere-2026-3722
Preprint. Discussion started: 27 July 2026

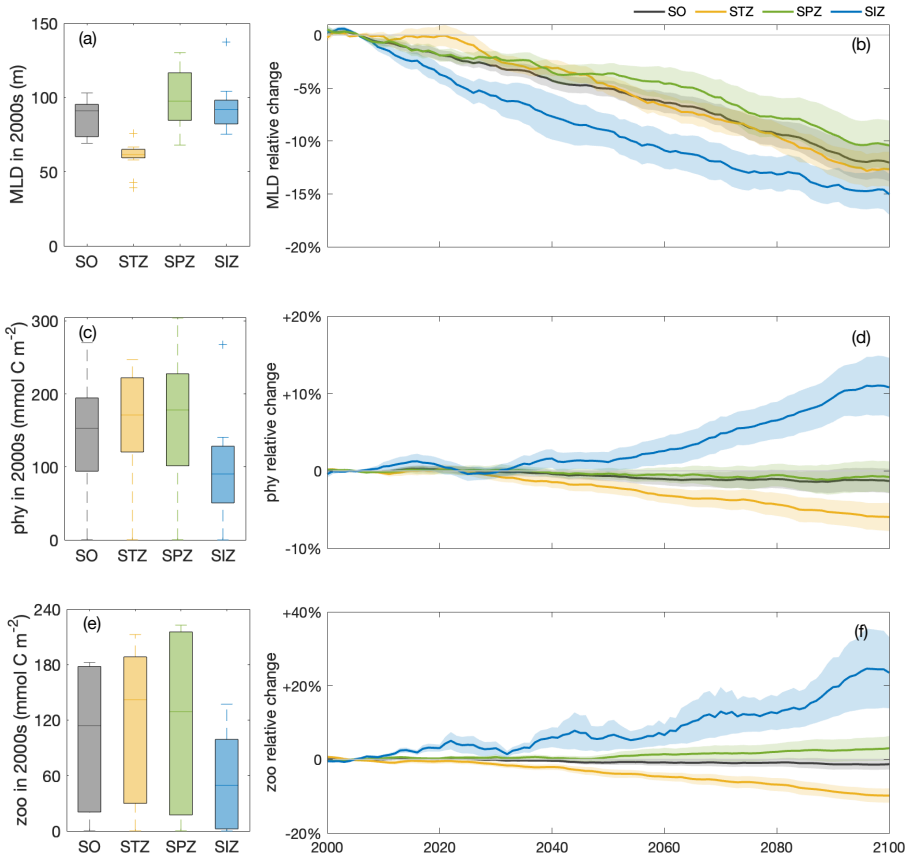

Figure 3. Modelled contemporary and future states over the 21st century from the MME (listed in Table 1) of (a, b) mixed layer depth (MLD), (c, d) phytoplankton (phy), and (e, f) zooplankton (zoo) biomass across the entire Southern Ocean (SO, black), the subtropical zone (STZ, yellow), the subpolar zone (SPZ, green), and the seasonal ice zone (SIZ, blue). Left panels (a, c, e) show the first decade of the 21st century (2000-2009) derived from the MME. Lines and boxes indicate the median and the 25th and 75th percentiles, respectively. The whiskers extend to the most extreme data points not considered outliers, and the outliers are plotted as '+'. Right panels (b, d, f) show projections of relative changes for 2000–2100 under the SSP5-8.5 scenario relative to the mean values of the first decade shown in (a, c, e). The solid lines in (b, d, f) indicate means, and the shadings indicate one standard error of the MME. The time series are filtered using a 10-year moving average. Please note the different vertical scales.

https://doi.org/10.5194/egusphere-2026-3722
Preprint. Discussion started: 27 July 2026

for plankton biomass, vary substantially across the multimodel ensemble, we first normalize the seasonal variations from each individual model by dividing them by their respective annual-means, so that the seasonal cycles of the different models become comparable. After normalization, we calculate the seasonality of the absolute changes by multiplying the multimodel mean annual value by the mean relative seasonality. This method is applied consistently across all variables in the budget analysis (Eqs. 5 and 6) in section 3.2. The processes included in "other processes" for phytoplankton (O_{phy}) and zooplankton (O_{zoo}) vary greatly among models and are typically not archived in CMIP simulations. Thus, we cannot fully close the phytoplankton and zooplankton budgets. Instead, we calculate O_{phy} and O_{zoo} as residuals of the respective biomass budgets. For phytoplankton, "other processes" (O_{phy}) include physical transport and additional loss terms such as non-consumptive mortality, aggregation, and sinking. Similarly, for zooplankton, "other processes" (O_{zoo}) could include physical transport, mortality, and metabolic losses.

To understand how plankton seasonality is changing over the century, we look into the change of the monthly tendencies over the course of the century (ΔT) for both phytoplankton (ΔT_{phy}, Eq. 7) and zooplankton (ΔT_{zoo}, Eq. 8):

$$\begin{aligned}\Delta \mathrm{T}_{\text{phy}} &= \frac{\mathrm{d}\,\mathrm{phy}_{2090s}}{\mathrm{d}t} - \frac{\mathrm{d}\,\mathrm{phy}_{2000s}}{\mathrm{d}t} = (PP_{2090s} - PP_{2000s}) - (GRAZ_{2090s} - GRAZ_{2000s}) - (O_{phy,2090s} - O_{phy,2000s}) \\ &= \Delta PP - \Delta GRAZ - \Delta O_{\text{phy}} \end{aligned} \tag{7}$$

$$\begin{aligned}\Delta \mathrm{T}_{\text{zoo}} &= \frac{\mathrm{d}\,\mathrm{zoo}_{2090s}}{\mathrm{d}t} - \frac{\mathrm{d}\,\mathrm{zoo}_{2000s}}{\mathrm{d}t} = (GRAZ_{2090s} - GRAZ_{2000s}) - (O_{zoo,2090s} - O_{zoo,2000s}) \\ &= \Delta GRAZ - \Delta O_{\text{zoo}} \end{aligned} \tag{8}$$

The change of the monthly tendencies over the century ΔT quantify how the rate of change of biomass between months shifts between the beginning and end of the century. If $\Delta T_{\text{phy}} > 0$ in a given month, the phytoplankton tendency for a month at the end of the century is more positive (or less negative) than at the beginning, meaning that this month contributes to a relative accumulation of biomass compared to the early-century baseline. Conversely, $\Delta T_{\text{phy}} < 0$ indicates that this month contributes to a relative loss. Whether this results in an amplification or damping of the seasonal cycle depends on the sign of the monthly biomass anomaly in the 2000s: in a month where end-of-century biomass already exceeds the beginning-of-century biomass, a positive ΔT implies the difference is growing larger; in a month where end-of-century biomass is already lower, a positive ΔT implies the deficit is shrinking. The same logic applies to ΔT_{zoo}. By decomposing ΔT into its contributing terms, ΔPP, $\Delta GRAZ$, and ΔO, we can attribute the monthly tendency change to specific biological processes, thereby identifying the mechanisms responsible for amplification or damping of the seasonal signal over the century.

The ΔT framework also provides the mechanistic basis for understanding when and why trophic amplification emerges seasonally. We define the *amplified period* as the months in which the monthly relative change of zooplankton biomass over the century exceeds both the annual-mean relative change and the corresponding monthly relative change of phytoplankton. The amplified period thus identifies the seasonal window where the disproportionate response of zooplankton relative to phytoplankton is most pronounced, and where the trophic amplification signal is concentrated. While the amplified period is defined by the outcome comparison between trophic levels, the budget decomposition of ΔT_{zoo} into $\Delta GRAZ$ and ΔO_{zoo} reveals

https://doi.org/10.5194/egusphere-2026-3722
Preprint. Discussion started: 27 July 2026

the specific processes responsible for driving this disproportionate seasonal response. Throughout this study, the long-term annual-mean analyses presented in Sect. 3.1 are based on the full MME of 12 models, whereas the seasonal budget decomposition analyses in Sect. 3.2 are restricted to the 7 models that archive both phytoplankton production and zooplankton grazing fluxes in their output (models marked † in Table 1). The strong agreement between the full MME and the flux-output subset in their projected relative changes (in Sect. 3.2) provides confidence that the seasonal analyses are representative of the broader ensemble.

3 Results

3.1 Long-term mean-state plankton response to changing climate

Over the 21st century, projected plankton biomass averaged across the whole Southern Ocean stays stable (black lines in Fig. 3d & f). For the current climate, estimates of mean phytoplankton and zooplankton biomass show comparatively larger spreads than estimates of physical MLD across MME members (Fig. 3a, c & e). Despite this spread in absolute biomass, the MME shows relatively strong agreement in relative changes of future projections. To analyse long-term trends, we examine simulated annual-means over the 21st century relative to the baseline climate conditions of the 2000s. During the 21st century, MLD is projected to shoal by $12 \pm 2\%$ across the entire Southern Ocean (Fig. 3b, black line), likely due to increasing ocean surface warming and subsequent stratification, while phytoplankton and zooplankton show little discernible change ($-1 \pm 2\%$ and $-1 \pm 1\%$, respectively). Nevertheless, underlying this apparent stability in Southern Ocean plankton lie opposing regional changes induced by diverse physical and ecological mechanisms.

3.1.1 Subtropical zone (STZ): negative trophic amplification

Total phytoplankton in the STZ is projected to decrease by $6 \pm 2\%$ over the 21st century (Fig. 3d, yellow line), along with decreasing primary production and zooplankton grazing (Fig. B1). The MME projects that the MLD will shoal by $12 \pm 2\%$ (Fig. 3b) over the century. Although annual-mean primary productivity and total zooplankton grazing flux decrease, phytoplankton growth rates and grazing mortality rate remain relatively stable (Fig. B2). Projected shoaling of the surface mixed layer likely enhances nutrient limitation while increasing phytoplankton exposure to light, with little net change in growth rate. The stability of the grazing mortality from zooplankton could be attributed to the positive effects of higher temperatures on zooplankton grazing (a feature implemented in nearly half of the models in our MME, for details see Rohr et al., 2023), which counterbalances the decline in phytoplankton concentration (Fig. B3a). Consequently, the decline in phytoplankton biomass is likely either driven by increased losses beyond zooplankton grazing or cannot be fully understood by analysing mean-state data alone. The seasonal analysis in Sect. 3.2.1 reveals that the mechanisms behind this decline differ across seasons. The phytoplankton decline is concentrated in the austral spring and summer and is primarily driven by nutrient limitation. This decline in phytoplankton biomass is consistent with previous findings in the subtropical zone (Leung et al., 2015; Cabré et al., 2015) and aligns with the expected trends in oligotrophic regions under climate change (Doney, 2006).

https://doi.org/10.5194/egusphere-2026-3722
Preprint. Discussion started: 27 July 2026

The concomitant relative decline in zooplankton biomass is projected to be $10 \pm 2\%$ (Fig. 3f), which is 67% more than that of phytoplankton, indicating negative trophic amplification (amplified relative decline along the food chain, Chust et al., 2014) over the 21st century. The amplified decline in zooplankton biomass results from both reduced zooplankton grazing flux (7%, Fig. B1), driven by declining phytoplankton concentration (6%, Fig. B3a), and likely also increased losses, such as higher metabolic costs associated with rising temperatures (Ratnarajah et al., 2023). Although warming may also enhance the zooplankton grazing rate, reduced phytoplankton availability outweighs the benefits of increased temperature, as the net outcome is a decline in grazing. This negative trophic amplification under climate change agrees with previous findings in oligotrophic regions (Chust et al., 2014; Kwiatkowski et al., 2019).

3.1.2 Subpolar zone (SPZ): no clear change

Within the SPZ, no clear change is projected for total phytoplankton over the century ($-1 \pm 2\%$, Fig. 3d, green line). From a bottom-up perspective, as this region is predominantly light- and iron-limited in the current climate (Arteaga et al., 2020), the shoaling mixed layer ($10 \pm 2\%$, Fig. 3b) improves light conditions, with surface iron projected to remain relatively stable (Fig. B4b, albeit future changes of iron supply are highly uncertain). Overall, phytoplankton production is projected to increase by 6% over the century (Fig. B1a), which agrees with the direction of change from recent observations (Liniger et al., 2025). However, the shoaling mixed layer also leads to an increase in surface phytoplankton concentration (5%, Fig. B3a), and hence intensified zooplankton grazing (7%, Fig. B1b). The dynamic balance between bottom-up and top-down processes keeps phytoplankton biomass relatively steady under projected climate change (Xue et al., 2024b).

Despite the noticeable increase in zooplankton grazing, zooplankton is projected to change little over the century ($3 \pm 3\%$, Fig. 3f). One would expect the increased zooplankton grazing to lead to a similar increase in zooplankton biomass. However, this positive effect appears to be balanced by higher metabolic or other losses, perhaps caused by a rise of mixed-layer temperatures. We note that directly attributing these losses is not possible with currently archived CMIP6 output, as zooplankton respiration and mortality fluxes are not routinely saved.

3.1.3 Seasonal ice zone (SIZ): positive trophic amplification

Within the SIZ, phytoplankton is projected to increase by $11 \pm 4\%$, due to substantially improved growth conditions, partially due to strong shoaling ($15 \pm 2\%$) in MLD over the century (Fig. 3b & d). Phytoplankton are mostly light-limited in this zone, owing to extensive sea ice coverage and regionally deep mixed layers (Arteaga et al., 2020). Consequently, the shoaling mixed layer along with sea ice retreat (more than 50% over the century, Fig. B5) increases both phytoplankton production (16%, Fig. B1a) and biomass, despite a concomitant increase in zooplankton grazing (30%, Fig. B1b).

Total zooplankton biomass is projected to increase by $23 \pm 10\%$, which is almost twice the increase of phytoplankton over the century (Fig. 3f), indicating positive trophic amplification (amplified increase along the food chain, Chust et al., 2014). The increase in total phytoplankton, along with the shoaling of the mixed layer, is expected to enhance the prey-predator encounter as a result of increasing phytoplankton concentration (21%, Fig. B3a), and hence zooplankton grazing (Fig. B1b

https://doi.org/10.5194/egusphere-2026-3722
Preprint. Discussion started: 27 July 2026

& Fig. B2b). Consequently, the zooplankton response is amplified compared to the projected changes in phytoplankton under climate change.

3.2 Seasonal mechanisms underlying the long-term mean-state changes

3.2.1 Seasonal nutrient limitation drives negative trophic amplification in the STZ

The projected annual-mean decline in phytoplankton ($6 \pm 2\%$) and the disproportionately larger decline in zooplankton ($10 \pm 2\%$) in the STZ (Sect. 3.1.1) emerge from a seasonally concentrated response rather than a uniform year-round trend. Under the current climate, STZ phytoplankton biomass peaks when the MLD starts to shoal and then declines as the MLD further shoals, a pattern that is broadly reproduced by the MME (Fig. 4a,c). Zooplankton tracks phytoplankton dynamics with a one-month lag (Fig. 4d), reflecting the tight prey–predator coupling that ultimately amplifies the zooplankton response under climate change.

Under projected climate change, both phytoplankton and zooplankton decline year-round, but the magnitude of the decline is strongly seasonally dependent. The most pronounced phytoplankton decrease occurs in October, when the MLD is shoaling rapidly and biomass is near its seasonal peak, whereas zooplankton show their greatest decline in austral summer (January and February), when the MLD is seasonally shallowest (Fig. 4d). During the amplified period (red shading in Fig. 4), zooplankton biomass decreases nearly three times as much as phytoplankton, representing a seasonal trophic amplification signal that is approximately 50% stronger than the signal revealed by the annual-mean changes. During the austral summer, the core of the amplified period, zooplankton biomass decreases by about four times as much as phytoplankton, nearly doubling the annual-mean trophic amplification signal. This seasonally concentrated response during austral spring and summer is the primary source of the annual-mean negative trophic amplification identified in Sect. 3.1.1.

The phytoplankton decline during the amplified period, particularly around its core in austral summer, is attributable to reduced primary production driven by MLD shoaling-induced nutrient limitation. During the amplified period, the phytoplankton budget (Fig. 4e) indicates that the biomass decline is dominated by reduced primary production ($\Delta PP < 0$), further reinforced by residual loss processes ($\Delta O_{\text{phy}} < 0$). The reduction in primary production can be further attributed either to a lower phytoplankton biomass as a result of increasing grazing mortality (g) or to deteriorating growth conditions, reflected in a lower growth rate (μ). Although annual-mean growth rates and grazing mortality remain broadly stable over the century (Fig. B2), their seasonal responses diverge substantially, ranging from -4% to $+10\%$ for growth rate and from -6% to $+14\%$ for grazing rate (Fig. 4b). Around the core amplified period, growth conditions deteriorate as mixed-layer shoaling under climate change accentuates nutrient limitation (lower left quadrant, Fig. 4b), driving a reduction in phytoplankton biomass. During the rest of the year, enhanced grazing mortality outweighs the enhanced phytoplankton growth rate (upper right quadrant, Fig. 4b), causing the phytoplankton biomass to continue declining.

The disproportionate zooplankton decline during the amplified period, which ultimately gives rise to negative trophic amplification, is driven by a reduction in grazing flux resulting from the concurrent decline in phytoplankton biomass. Although zooplankton biomass declines year-round, this decline is primarily attributable to elevated losses (ΔO_{zoo}, e.g., increased metabolic costs under warming) during the non-amplified period, whereas it is governed by a sharp reduction in zooplankton grazing

https://doi.org/10.5194/egusphere-2026-3722
Preprint. Discussion started: 27 July 2026

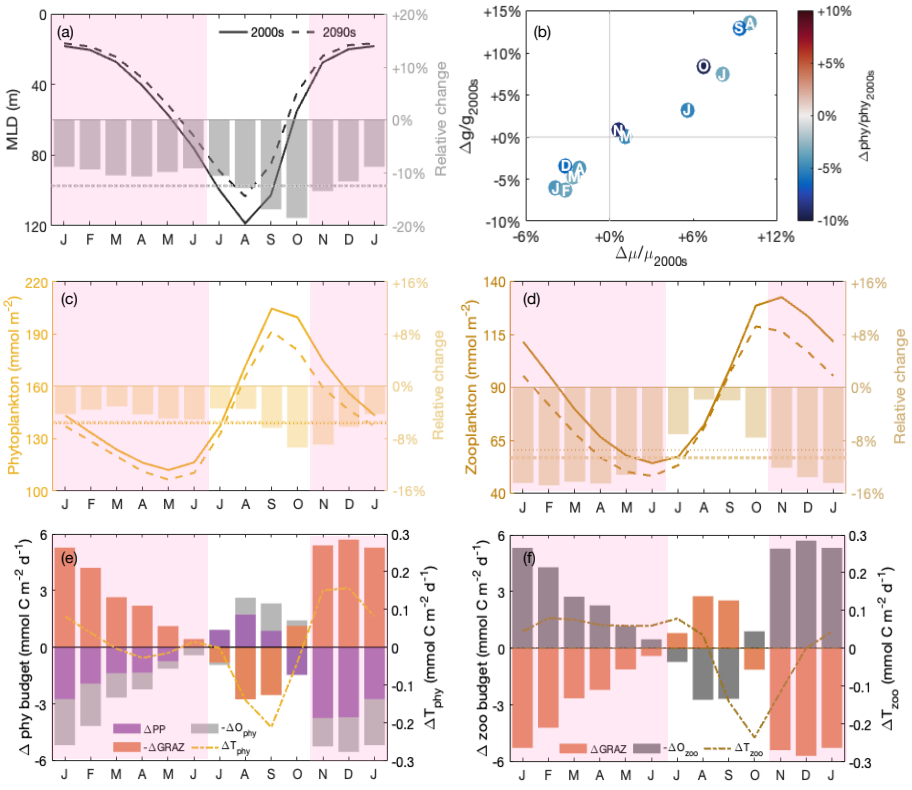

Figure 4. Seasonality of the subtropical zone (STZ). Absolute seasonality (left axis, present: solid line, future: dashed line) and relative change with respect to the 2000s annual-mean (right axis, bars) of (a) mixed layer depth (MLD), (c) phytoplankton, and (d) zooplankton (mmol C m^{-2}). The dotted horizontal line indicates the projected annual-mean at the end of the century. (b) Changes in phytoplankton growth rate ($\Delta\mu/\mu_{2000s}$, Eq. 3) and zooplankton grazing mortality ($\Delta g/g_{2000s}$, Eq. 4) relative to their respective 2000s monthly means. Marker colors indicate the relative change in integrated phytoplankton biomass (Δphy/phy$_{2000s}$) and month abbreviations are labelled on each marker. Changes of (e) phytoplankton and (f) zooplankton budget terms (in mmol C m^{-2} d^{-1}, left axes) for each month at the end relative to the beginning of the century, and contributions of individual processes (Eqs. 5 & 6): ΔPP (purple), $-\Delta$GRAZ (orange), and $-\Delta O_{\mathrm{phy}}$ (grey) in panel (e), and ΔGRAZ (orange) and $-\Delta O_{\mathrm{zoo}}$ (grey) in panel (f). PP is primary production, $GRAZ$ is zooplankton grazing, O denotes other processes. The dashed orange line indicates ΔT_{phy} in (e) and ΔT_{zoo} in (f) (right axes). As the overall biomass change over the century is negative in the STZ, a positive ΔT in (e) and (f) indicates that the biomass decline is becoming less pronounced between months. Red-shaded periods in all panels indicate the seasonal window of trophic amplification, defined as months in which the monthly relative change of zooplankton exceeds both the annual-mean relative change and the corresponding monthly relative change of phytoplankton (see Sect. 2.4). Opposite signs of grazing in (e) and (f) reflect its role as a loss term for phytoplankton but a source term for zooplankton. All panels show results derived from models with flux output marked as † in Table 1. The light dotted horizontal lines in panels (c) and (d) show the projected end-of-century annual mean from the MME in Fig. 3, illustrating that this projected mean is largely insensitive to the specific MME used.

https://doi.org/10.5194/egusphere-2026-3722
Preprint. Discussion started: 27 July 2026

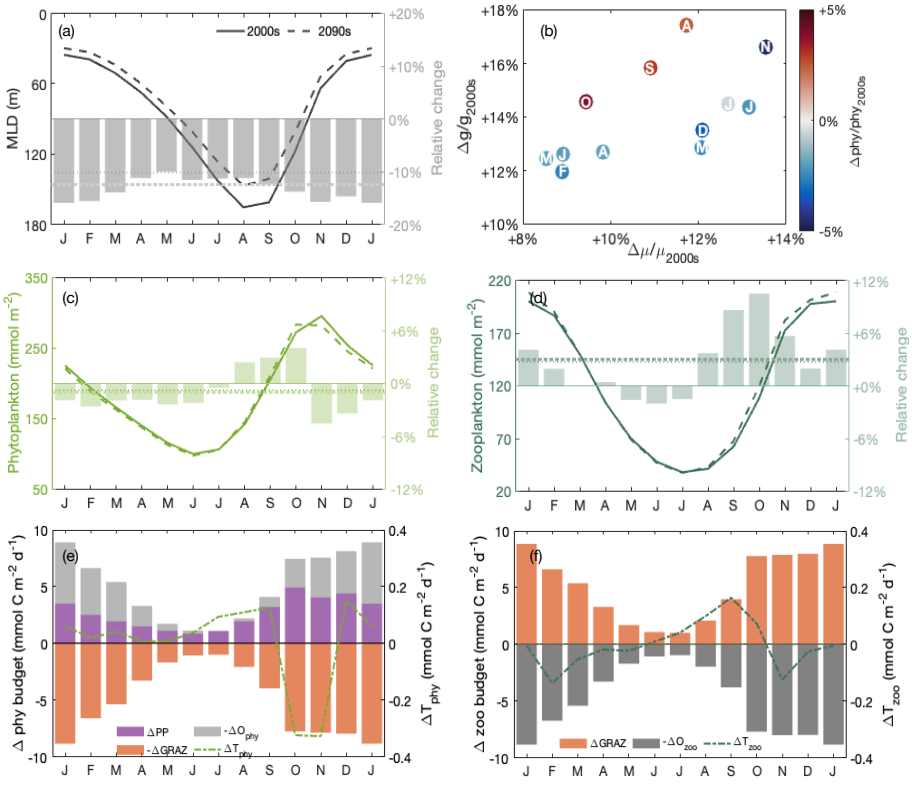

Figure 5. Same as Fig. 4 but for the subpolar zone (SPZ). Note the different scaling for the axes as compared to the STZ.

($\Delta GRAZ$) during the amplified period (Fig. 4f). During the amplified period, the decline in phytoplankton biomass reduces total prey availability, while the concurrent decrease in phytoplankton concentration (Fig. C1a), which is a by-product of the phytoplankton biomass decline, further reduces prey-predator encounter rates. Together, these changes cause the grazing flux to decline sharply and thereby amplify the decline in total zooplankton biomass.

3.2.2 Compensatory bottom-up and top-down changes stabilise plankton in the SPZ

The projected near-stability of both phytoplankton ($-1 \pm 2\%$) and zooplankton ($3 \pm 3\%$) in the SPZ (Sect. 3.1.2) emerges from the interplay of seasonally varying processes rather than from the absence of change (Fig. 5). Under the current climate, phytoplankton biomass peaks when the mixed layer shoals and light conditions improve, with zooplankton grazing catching up rapidly thereafter. Unlike in the STZ, where phytoplankton are predominantly macronutrient-limited, SPZ phytoplankton are constrained primarily by iron and light availability under the current climate (Arteaga et al., 2020; Moore et al., 2013; Weis et al., 2024), a distinction that proves consequential for how this zone responds to climate change.

Under projected climate change, phytoplankton growth rate (μ) improves throughout the year in the SPZ, ranging from $+9\%$ to $+14\%$ over the century (Fig. 5b), in contrast to the seasonally deteriorating growth conditions in the STZ. Similarly, grazing

https://doi.org/10.5194/egusphere-2026-3722
Preprint. Discussion started: 27 July 2026

mortality from zooplankton (g) increases year-round by $+12\%$ to $+17\%$ (Fig. 5b). The seasonal structure of these changes is governed by the MLD regime. From August to October, enhanced phytoplankton production driven by mixed-layer shoaling-induced light improvement and rising temperatures leads to a subtle increase in phytoplankton biomass (Fig. 5e). For the rest of the year, mixed-layer shoaling elevates surface phytoplankton concentration and temperature, intensifying zooplankton grazing and causing a subtle decline in phytoplankton biomass (Fig. 5c). Despite these opposing seasonal tendencies, their magnitudes are modest relative to those in the STZ and SIZ, and no single season dominates sufficiently to produce a net annual trend, resulting in broadly stable phytoplankton biomass over the century.

The zooplankton response mirrors this seasonal balance. Although zooplankton benefit from improved grazing conditions year-round, increasing loss terms offset the higher grazing intake across all seasons (Fig. 5c,f). The increasing losses likely reflect elevated metabolic costs under warming, although direct attribution is limited by the lack of routinely archived zooplankton loss fluxes in CMIP6 output. Neither the gains nor the losses dominate at any particular time of year, preventing the emergence of a seasonally-concentrated amplification window analogous to those identified in the STZ and SIZ. Consequently, the compensatory balance between bottom-up and top-down processes for phytoplankton, and between grazing gains and losses for zooplankton, is maintained throughout the seasonal cycle, resulting in near-stable long-term annual means and the absence of trophic amplification (Fig. 3).

3.2.3 Spring and summer light availability drives positive trophic amplification in the SIZ

The projected annual-mean increase in phytoplankton ($11 \pm 4\%$) and the disproportionately larger increase in zooplankton ($23 \pm 10\%$) in the SIZ (Sect. 3.1.3), analogous to the STZ but of opposite sign, emerge from a seasonally concentrated response rather than a uniform year-round trend. Under the current climate, phytoplankton biomass in the SIZ is governed primarily by light availability, which is regulated by solar irradiance, sea-ice extent, and MLD. Minimal phytoplankton biomass persists through the austral winter because of extremely low light conditions, before rising sharply toward a January peak that coincides with the shallowest MLD (Fig. 6a,c). Zooplankton tracks phytoplankton dynamics with a one-month lag (Fig. 6c), and the MME reproduces the relative seasonal variability of both groups reasonably well despite some discrepancies in absolute biomass. This strong light-driven seasonal cycle, absent in the STZ and less pronounced in the SPZ, sets the stage for the disproportionate zooplankton response to climate change described below.

Under projected climate change, both phytoplankton and zooplankton increase throughout most of the year, with only a minor decline during the winter months, when light availability remains extremely low. As in the STZ, phytoplankton exhibit their most pronounced increases in September and October, when the MLD is shoaling rapidly and biomass is approaching its annual peak (Fig. 6c). Zooplankton subsequently show their largest increase in October and November, following the phytoplankton increase (Fig. 6d). During the amplified period from October to January, zooplankton biomass increases by more than four times as much as phytoplankton biomass, which is more than twice the annual-mean trophic amplification signal. This identifies austral spring and summer as the seasons in which positive trophic amplification is concentrated and from which the annual-mean signal primarily arises (red shading, Fig. 6d–f). The core of the amplified period occurs in January, during

https://doi.org/10.5194/egusphere-2026-3722
Preprint. Discussion started: 27 July 2026

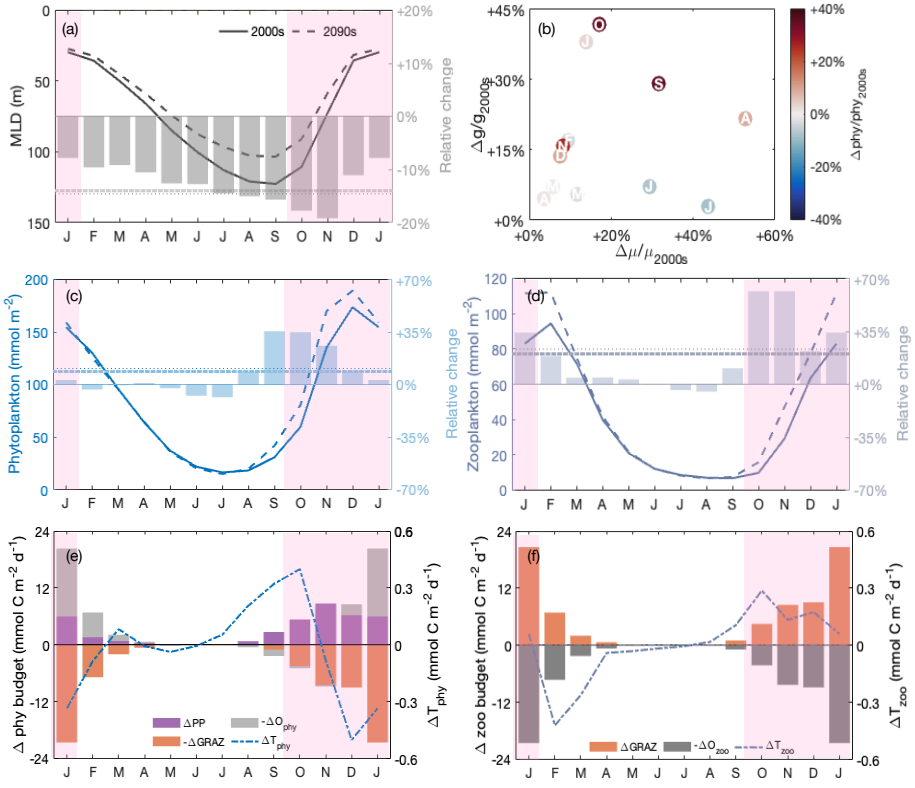

Figure 6. Same as Fig. 4 but for the SIZ. Note that plankton biomass difference over the century is positive—indicating that the biomass at the end of the century is higher than at the beginning—a positive Δnet flux in (e) and (f) suggests that the difference is becoming more pronounced in (c) and (d). Also the scaling is different for the axes as compared to the STZ and SPZ.

austral summer, when zooplankton biomass increases by more than eleven times as much as phytoplankton biomass, exceeding five times the annual-mean signal.

Positive trophic amplification during austral spring and summer is driven by enhanced zooplankton grazing, which results from increased phytoplankton growth due to improved light availability and biomass compression caused by mixed-layer shoaling under climate change. Increased phytoplankton production, together with reduced non-attributable losses, more than compensates for elevated grazing, leading to higher phytoplankton biomass throughout most of the year (Fig. 6d,e). Phytoplankton growth rates and grazing mortality are projected to increase year-round, as in the SPZ, but to a much greater extent, ranging from $+4\%$ to $+53\%$ and from $+3\%$ to $+42\%$, respectively (Fig. 6b). Accordingly, the increase in phytoplankton biomass, particularly during the amplification period (red shading in Fig. 6), is dominated by enhanced phytoplankton growth, likely driven by improved light conditions associated with mixed-layer shoaling, sea-ice retreat (Fig. B5), and rising temperatures. The increase in zooplankton biomass can be attributed to enhanced grazing (Fig. 6f), driven by greater food availability from higher integrated phytoplankton biomass (Fig. C1) and by higher prey-predator encounter rates resulting from elevated phytoplankton concentration. The elevated grazing intake more than compensates for the higher non-attributable losses (Fig. 6f),

https://doi.org/10.5194/egusphere-2026-3722
Preprint. Discussion started: 27 July 2026

leading to an overall increase in zooplankton biomass. Strong amplification during the amplified period produces a pronounced long-term increase in zooplankton biomass relative to phytoplankton, resulting in positive trophic amplification on an annual scale.

4 Discussion and Conclusion

This study demonstrates that trophic amplification in the Southern Ocean is fundamentally a seasonal phenomenon, driven by unevenly distributed changes across the annual cycle rather than uniform long-term trends. Beneath the seemingly stable Southern Ocean plankton dynamics lie not only opposing regional trends (Leung et al., 2015; Deppeler and Davidson, 2017) but also seasonally concentrated responses whose intensity substantially exceeds that of the annual-mean signal. In both the STZ and the SIZ, trophic amplification emerges primarily during austral spring and summer, when mixed-layer shoaling accentuates nutrient limitation and enhances light availability (Behrenfeld, 2010; Xue et al., 2022b), thereby driving disproportionate zooplankton responses through changes in prey concentration and encounter efficiency (Xue et al., 2022a; Stock et al., 2014). This seasonal concentration means that assessments of climate-change impacts on Southern Ocean plankton based on annual-mean projections alone will systematically underestimate the magnitude and potentially also the ecological severity of trophic amplification (Chust et al., 2014; Kwiatkowski et al., 2019; Lotze et al., 2019). The seasonal concentration occurs precisely in the most critical season for coupling among the different trophic levels in the broader marine food web (Cushing, 1975; Xue and Hill, 2025; Asch et al., 2019; Edwards and Richardson, 2004). Our results, therefore, underscore the need to move beyond mean-state assessments toward a regionally and, more importantly, seasonally resolved understanding of how climate change restructures trophic interactions in the Southern Ocean and beyond.

The projected spatially diverse patterns of trophic amplification are broadly consistent with earlier work based on CMIP5 and more recent models (Kwiatkowski et al., 2019; Atkinson et al., 2024), confirming the robustness of the trophic amplification signal across successive model generations. The three key food web properties identified by Stock et al. (2014): zooplankton growth efficiency (ZGE), the trophic level of zooplankton, and zooplankton-phytoplankton coupling (ZPC), remain relevant here, with our findings particularly emphasising the role of ZPC as the proximate driver of seasonal trophic amplification in both the STZ and SIZ, consistent with the seasonal-scale analysis of Xue et al. (2022a). The disproportionate zooplankton response in both zones is ultimately mediated by changes in phytoplankton concentration rather than integrated biomass alone, highlighting the importance of physical forcing in driving zooplankton-phytoplankton coupling as a mechanism linking the physical environment to trophic transfer (Behrenfeld, 2010; Xue et al., 2022a, 2024a). While the role of ZGE is more difficult to isolate (zooplankton respiration and mortality fluxes are not routinely archived in CMIP6 output, Rohr et al., 2023), the seasonal decomposition of zooplankton loss terms suggests a seasonally variable contribution also for ZGE that warrants further investigation. If heterotrophic processes are more temperature-sensitive, that could disproportionately benefit higher trophic levels relative to primary producers (Archibald et al., 2022) and reinforce the positive trophic amplification projected in the SIZ but partially counteract the negative amplification in the STZ. Kwiatkowski et al. (2019) pointed out that flexible stoichiometry in phytoplankton and zooplankton can introduce further complexity to trophic interactions, potentially intensifying negative

https://doi.org/10.5194/egusphere-2026-3722
Preprint. Discussion started: 27 July 2026

trophic amplification under future climate conditions. Flexible stoichiometry is not represented in most models within our MME and, therefore, is a potential source of underestimation in the STZ projections. Notably, the UVic-OPEM model employs an optimality-based framework that implicitly captures flexible stoichiometry (Pahlow et al., 2020), and its broadly consistent projections with the rest of the MME suggest that this source of uncertainty may not fundamentally alter the sign or spatial pattern of trophic amplification identified here, though its magnitude in the STZ may still be underestimated.

A further structural limitation of the models used here concerns the representation of food web architecture in the Southern Ocean. Observational evidence indicates that the Southern Ocean food web is characteristically "top-heavy", with zooplankton biomass equalling phytoplankton biomass (Yang et al., 2022; Shurin et al., 2006), a feature that none of the models in our MME reproduce (Fig. 2g–i). This systematic bias likely reflects an underestimation of top-down control in current Earth system models, which may arise from the limited number of zooplankton functional types represented (Table 1) or insufficient representation of zooplankton omnivory (McCauley et al., 2018). Stronger top-down control than currently modelled would imply a tighter zooplankton-phytoplankton coupling, which, given that ZPC is identified here as the proximate driver of seasonal trophic amplification, could amplify both the positive and negative trophic amplification signals beyond what our MME projects. Encouragingly, our analysis suggests that the projected relative changes in plankton biomass across the three zones are not systematically influenced by the structural complexity of the ecosystem models within the MME (Fig. C4). This means the broad trophic amplification patterns identified here are robust to differences in model complexity, even if their absolute magnitudes remain uncertain. Nevertheless, the development of Earth system models capable of reproducing the observed top-heavy food web structure of the Southern Ocean remains an important priority, as the systematic underestimation of top-down control represents a potentially significant source of bias in projections of trophic amplification and higher trophic level responses to climate change (Rohr et al., 2023).

Beyond the biological uncertainties discussed above, a key physical uncertainty in our projections concerns the future trajectory of mixed-layer depth, which is the central mechanism linking physical forcing to trophic amplification throughout this study. Our MME projects a year-round shoaling of the MLD across all three Southern Ocean zones under the SSP5-8.5 scenario, consistent with the expected increase in upper-ocean stratification under warming (Kwiatkowski et al., 2020). However, recent observations suggest a trend of summertime mixed-layer deepening despite increasing stratification (Sallée et al., 2021), a finding that diverges from our MME projections and from the physical reasoning underpinning the seasonal amplification mechanism identified here. This discrepancy is particularly consequential given that the trophic amplification signal in both the STZ and SIZ emerges primarily during summertime. If summertime MLD trends are in reality positive rather than negative, the seasonal window of amplification identified here could be narrower, weaker, or shifted in timing relative to our projections. Despite this, the MME reproduces the relative amplitude of MLD seasonality reasonably well under the current climate (Fig. 2a–c), providing some confidence that the seasonal mechanisms identified here are physically grounded, even if the magnitude of future MLD shoaling remains uncertain.

Despite these uncertainties, the seasonal concentration of trophic amplification during austral spring and summer has potential for far-reaching consequences for higher trophic levels that are likely to be robust across a range of plausible MLD trajectories. This seasonal period coincides with the critical window for fish recruitment, larval feeding, and the transfer of energy

https://doi.org/10.5194/egusphere-2026-3722
Preprint. Discussion started: 27 July 2026

to larger consumers (Cushing, 1975; Edwards and Richardson, 2004), meaning that the projected changes in plankton biomass and seasonality are likely to have disproportionate ecological consequences relative to what annual-mean changes would suggest. Our MME projects shifts in the timing of phytoplankton and zooplankton blooms across all three zones (Fig. C3), with different degrees and even directions of phenological shifts for zooplankton and for phytoplankton (which itself constitutes a form of trophic decoupling, Yamaguchi et al., 2022), raising the prospect of widening trophic mismatches between successive levels of the food web (Edwards and Richardson, 2004). The ecological consequences of such mismatches, however, are likely to differ fundamentally between zones. In the STZ, the combination of reduced plankton biomass and potential phenological mismatches represents a compounding risk: declining food availability weakens the buffer against temporal trophic mismatches (Gotceitas et al., 1996; Asch et al., 2019), potentially making the STZ marine ecosystem increasingly vulnerable in the changing climate. In contrast, the projected increase in plankton biomass in the SIZ during the productive spring and summer season may enhance the resilience of higher trophic levels to phenological mismatches. When sufficient prey is available, larval fish and other consumers are better able to compensate for temporal offsets in food availability (Gotceitas et al., 1996). This asymmetry between zones suggests that the ecological trajectories of the STZ and SIZ under climate change may diverge considerably, with the STZ facing a progressively more vulnerable food web and the SIZ potentially supporting enhanced productivity at higher trophic levels, at least through the mechanisms captured by current Earth system models. Explicitly incorporating the dynamics of fish and other high-trophic-level organisms into climate projections will be essential for a complete assessment of the ecological consequences identified here. Changes across trophic levels are tightly coupled through both top-down and bottom-up interactions, which can feed back on plankton and biogeochemical dynamics of the Southern Ocean (Sarmiento et al., 2004a; Le Quéré et al., 2016).

Overall, our results reveal that the seemingly stable Southern Ocean plankton biomass under climate change masks a complex mosaic of opposing regional and seasonal responses. In the STZ, future mixed-layer shoaling-induced nutrient limitation drives seasonally concentrated negative trophic amplification during austral spring and summer, progressively weakening the base of the food web during the most ecologically critical season. In the SIZ, future sea-ice retreat and mixed-layer shoaling enhance light availability that drives positive trophic amplification over the same period, potentially supporting enhanced productivity at higher trophic levels. In the SPZ, compensatory seasonal changes in bottom-up and top-down control yield no net trophic amplification, masking substantial seasonal reorganization beneath an apparently stable annual-mean. Across all three zones, the seasonal dimension of trophic amplification emerges as the critical lens through which climate-change impacts on Southern Ocean plankton need to be assessed. Annual-mean projections may not only underestimate the magnitude of trophic change but also obscure its seasonal timing, which ultimately determines its ecological consequences for the broader marine food web. These findings underscore the importance of regionally and seasonally resolved assessments of plankton dynamics for projecting the future of Southern Ocean ecosystems and the globally significant biogeochemical functions they sustain.

Data availability. All CMIP6 ESM output is available via the Earth System Grid Federation (https://esgf-data.dkrz.de). The FOCI model data are available through (Chien et al., 2022). The OPEM model data are available through (Pahlow et al., 2020). The observation-based

https://doi.org/10.5194/egusphere-2026-3722
Preprint. Discussion started: 27 July 2026

MLD data are available from the Argo mixed-layer database (http://mixedlayer.ucsd.edu/, Holte et al., 2017). BGC-ARGO data are available through OneArgo Float toolboxes (Frenzel et al., 2022).

https://doi.org/10.5194/egusphere-2026-3722
Preprint. Discussion started: 27 July 2026

Appendix A: Observational data for model validation

BGC-Argo float data, used in this study to assess the performance of the MME, have been obtained via the OneArgo Float toolboxes (Frenzel et al., 2022). These floats are equipped with an array of sensors, including conductivity-temperature-depth (CTD), oxygen, nitrate, pH, bio-optical sensors, etc. The selection of profiles was based on the presence of bio-optical sensors capable of measuring particulate backscattering at 700 nm (bbp(700)). The selected profiles span a period from 13 Sep 2010 to 4 Mar 2024, ensuring comprehensive coverage of the entire Southern Ocean across all months of the year (Fig. A1), which is essential for providing a robust representation of seasonal patterns under the current climate.

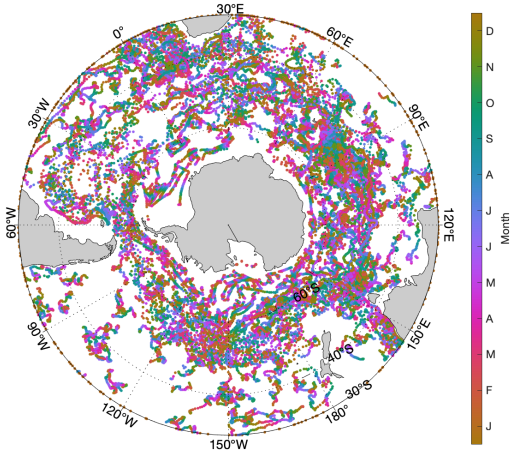

Figure A1. Tracks of BGC-Argo floats equipped with bio-optical sensors used in this study are color-coded by the month of the year when the data were collected.

Figure A2 illustrates the MLD distributions in three distinct Southern Ocean zones: the Subtropical (STZ), Subpolar (SPZ), and Seasonal Ice (SIZ) zones. Panels (a-l) feature simulated MLDs from models detailed in Table 1, while the bottom-right panel compares these with observed MLDs from Argo data (http://mixedlayer.ucsd.edu/).

Appendix B: Long-term mean-state changes: supporting figures

Figure B1 presents the long-term trends in depth-integrated primary production (PP) and zooplankton grazing flux (GRAZ) across the three Southern Ocean zones over the 21st century. These two flux processes are the primary drivers of the plankton biomass changes shown in Fig. 3, and their trends reflect the combined influence of changes in both biomass and specific rates, as shown in Fig. B2.

https://doi.org/10.5194/egusphere-2026-3722
Preprint. Discussion started: 27 July 2026

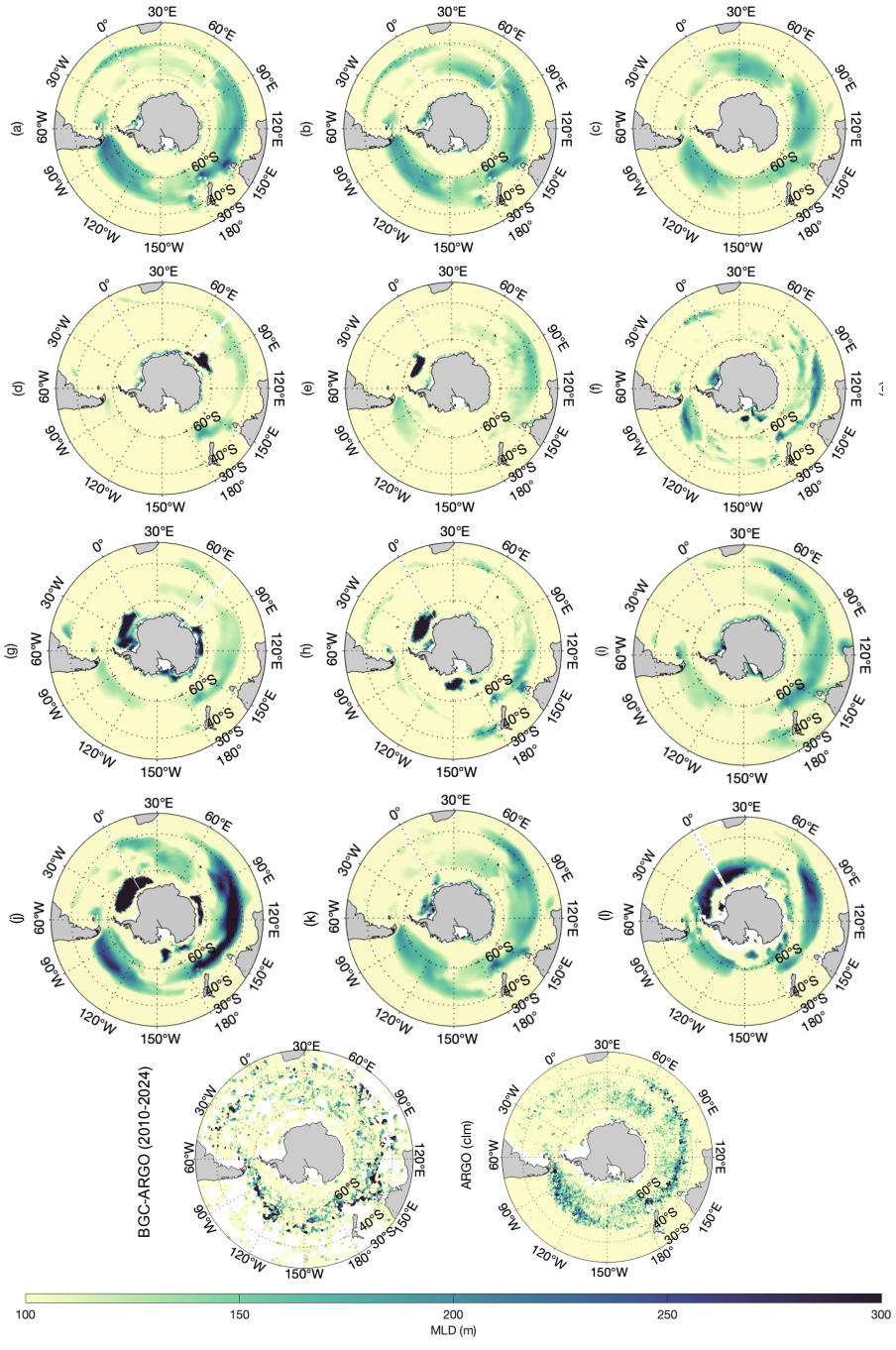

Figure A2. Contemporary MLD Maps in the Southern Ocean. Panels (a-l) display simulated MLD from models listed in Table 1. The two bottom-right panels depict observed interannual MLD during 2010-2024 obtained from BGC-Argo data (https://argo.ucsd.edu/data/data-from-gdacs/) and Argo mixed-layers product covering 2000 -2021 (https://mixedlayer.ucsd.edu/).

https://doi.org/10.5194/egusphere-2026-3722
Preprint. Discussion started: 27 July 2026

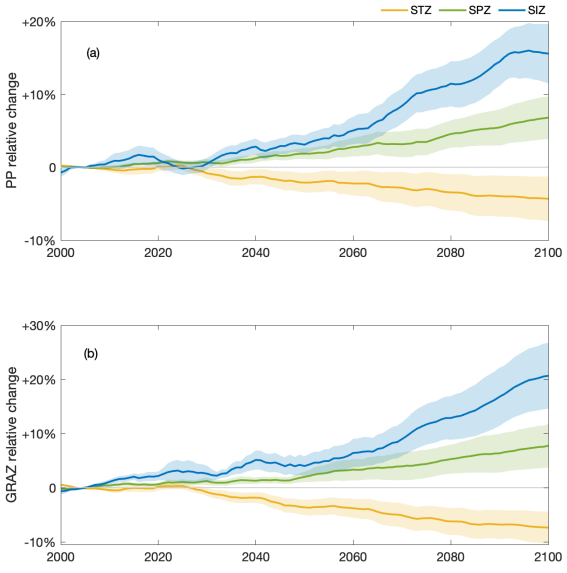

Figure B1. MME projections for the subtropical zone (STZ, yellow), subpolar zone (SPZ, green), and seasonal ice zone (SIZ, blue) of the relative changes of depth-integrated (a) primary production and (b) grazing flux by zooplankton from 2000 - 2100 under the SSP5-8.5 scenario, with the solid line indicating the mean of the MME and shading indicating one standard error of the MME, relative to the respective mean values of the first decade of the 21st century (2000-2009). The time series are filtered using a 10-year moving average.

Figure B2 presents the long-term trends in phytoplankton growth rate and zooplankton grazing mortality across the three zones, providing insight into the environmental factors driving changes in bottom-up and top-down control of plankton biomass under climate change.

Figure B3 presents the long-term trends in surface phytoplankton and zooplankton concentrations across the three zones. Although the study primarily focuses on vertically integrated biomass, surface concentration trends are essential for visualising the dilution and compression effects associated with increased stratification under climate change. For example, while vertically integrated phytoplankton biomass remains stable in the SPZ (Fig. 3d), surface concentration increases as the mixed layer shoals, with important consequences for zooplankton encounter rates and grazing.

B1 Iron and sea ice trends under climate change

Iron availability is an important limiting factor for phytoplankton growth and plankton community structure in the Southern Ocean (Moore et al., 2013; Arteaga et al., 2020). However, not all models in the MME include iron cycling explicitly (Table 1), and those that do show limited skill in reproducing the observed contemporary iron distribution (Tagliabue et al., 2016). Furthermore, projections of future iron supply remain highly uncertain, with iron limitation suggested to have increased over recent decades (Ryan-Keogh et al., 2023) while atmospheric iron supply is projected to increase in the future due to wildfires

https://doi.org/10.5194/egusphere-2026-3722
Preprint. Discussion started: 27 July 2026

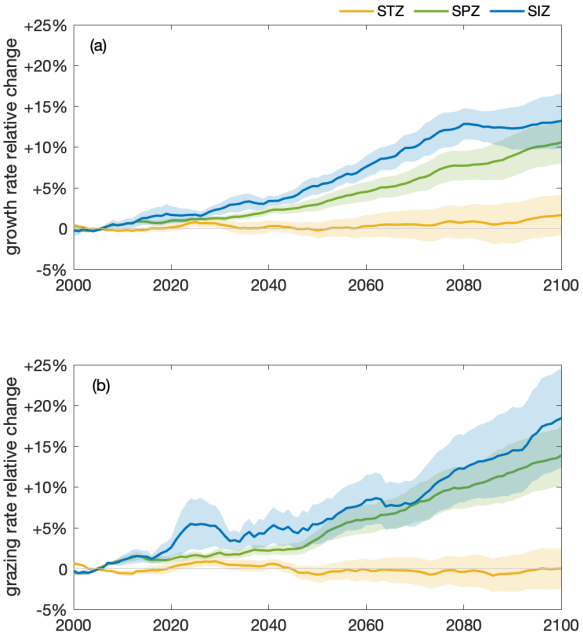

Figure B2. MME projections of the relative changes in depth-integrated (a) phytoplankton growth rate (primary production divided by phytoplankton biomass) and (b) zooplankton grazing mortality (grazing divided by phytoplankton biomass) from 2000–2100 under the SSP5-8.5 scenario. Colors, lines, and shading as in Fig. B1.

and escalating desertification (Bowman et al., 2020; Woodward et al., 2005; Hamilton et al., 2020). Our MME projects an increase in surface iron concentration in the STZ, a negligible trend in the SPZ, and a decrease in the SIZ over the century (Fig. B4), although considerable uncertainty is associated with all three projections.

Sea ice extent in the Southern Ocean is projected to decline by more than 50% by the end of the century (Fig. B5), representing a major additional driver of enhanced light availability in the SIZ beyond mixed-layer shoaling, and contributing directly to the positive trophic amplification projected in that zone (Sect. 3.2.3).

Appendix C: Seasonal plankton dynamics: supporting figures

Figures C1 & C2 provide supporting detail on the seasonal changes in phytoplankton surface concentration, depth-integrated primary production, and zooplankton grazing across the three Southern Ocean zones, elucidating the mechanisms driving the seasonal trophic amplification signals discussed in Sect. 3.2.

https://doi.org/10.5194/egusphere-2026-3722
Preprint. Discussion started: 27 July 2026

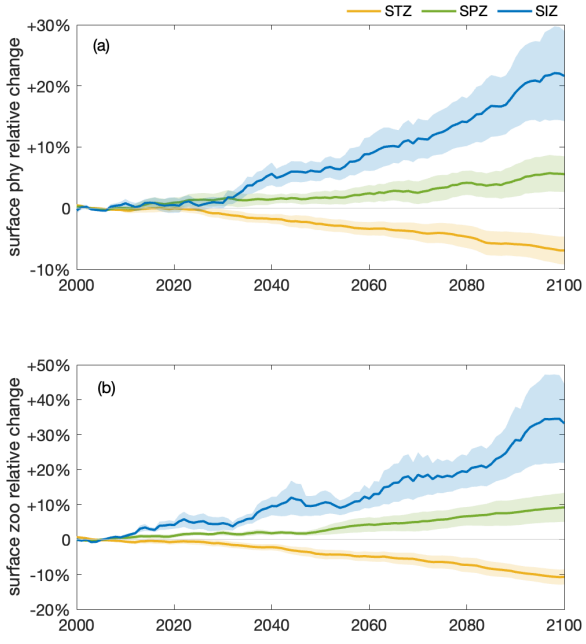

Figure B3. MME projections of the relative changes in surface concentration of (a) phytoplankton and (b) zooplankton from 2000–2100 under the SSP5-8.5 scenario. Colors, lines, and shading as in Fig. B1.

C1 Phenological shifts in plankton bloom timing

Figure C3 presents projected shifts in phytoplankton and zooplankton bloom timing across the three zones, characterised by changes in bloom initiation and termination dates defined following Behrenfeld et al. (2017) and Yamaguchi et al. (2022). Bloom initiation occurs when the biomass accumulation rate turns positive and termination when it becomes negative. The MME projects shifts in bloom timing particularly in the STZ and SIZ, with more pronounced phenological changes for zooplankton than for phytoplankton, raising the prospect of widening trophic mismatches as discussed in Sect. 4.

C2 Influence of ecosystem model structure and complexity on plankton projections

The MME encompasses a range of plankton ecosystem structures, including models with one to three phytoplankton functional types, one to three zooplankton functional types, and varying formulations of iron dynamics (Table 1). Fig. C4 demonstrates that neither the number of plankton functional types nor the explicit inclusion of iron limitation exerts a systematic influence on the projected changes in phytoplankton and zooplankton biomass within any of the three zones, supporting the robustness of the trophic amplification patterns identified in the main text.

https://doi.org/10.5194/egusphere-2026-3722
Preprint. Discussion started: 27 July 2026

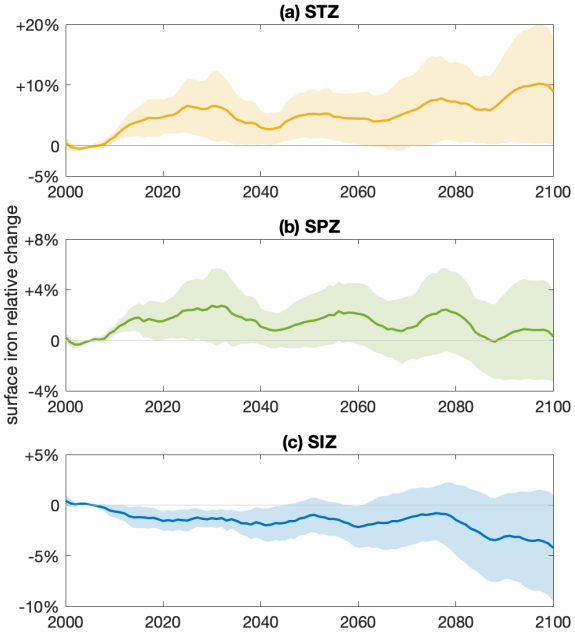

Figure B4. MME projections of the relative changes in dissolved iron concentration from 2000–2100 under the SSP5-8.5 scenario in the (a) STZ, (b) SPZ, and (c) SIZ. Solid lines indicate the MME mean, and shading indicates one standard error relative to the mean values of 2000–2009. Dissolved iron data are available only from models marked with * in Table 1. Time series are filtered using a 10-year moving average.

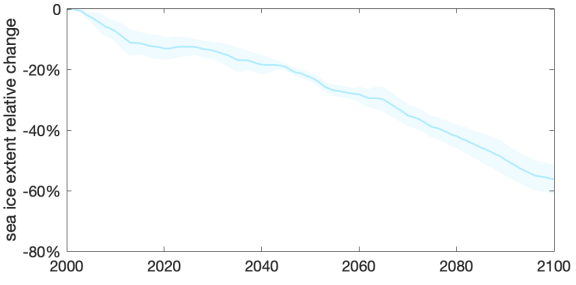

Figure B5. MME projections of the relative changes in sea ice extent from 2000–2100 under the SSP5-8.5 scenario, relative to the mean values of 2000–2009. Solid lines indicate the MME mean and shading indicates one standard error. Time series are filtered using a 10-year moving average. The model ensemble includes models marked with ‡ in Table 1.

https://doi.org/10.5194/egusphere-2026-3722
Preprint. Discussion started: 27 July 2026

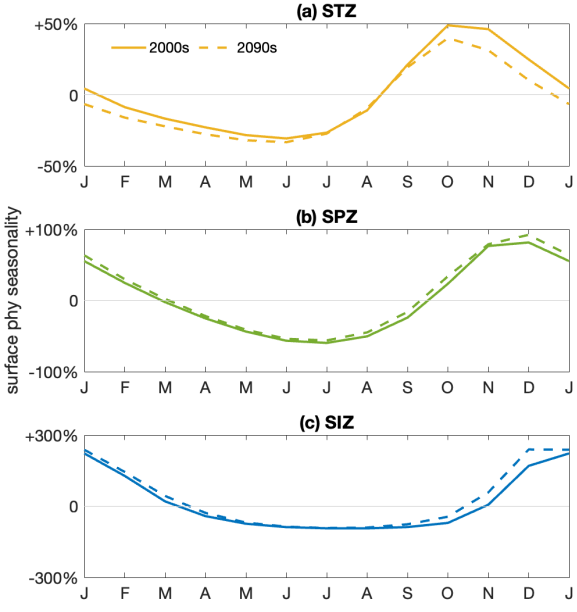

Figure C1. Present (2000s, solid) and future (2090s, dash) seasonalities of surface phytoplankton concentration in (a) STZ, (b) SPZ, and (c) SIZ, relative to the annual-mean of the first decade (2000-2009). Note the different scales of the vertical axes.

https://doi.org/10.5194/egusphere-2026-3722
Preprint. Discussion started: 27 July 2026

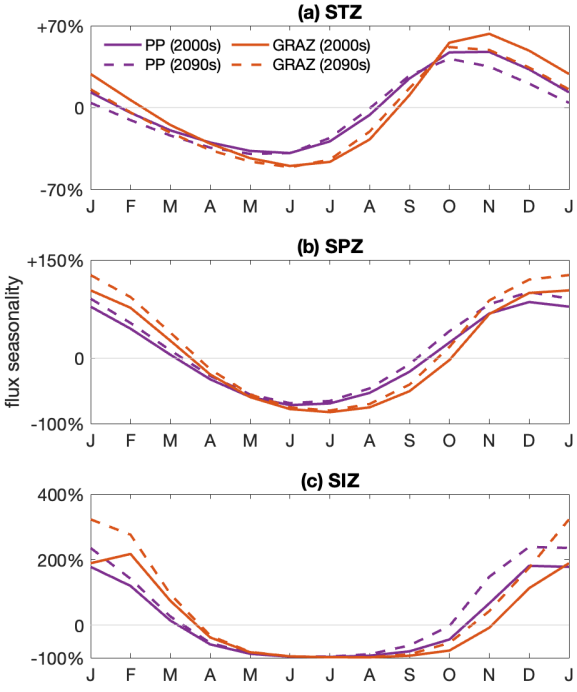

Figure C2. Present (2000s, solid) and future (2090s, dash) seasonalities of integrated phytoplankton production (purple) and zooplankton grazing (red) in (a) STZ, (b) SPZ, and (c) SIZ, relative to the annual-mean of the first decade (2000-2009). Note the different scales of the vertical axes.

https://doi.org/10.5194/egusphere-2026-3722
Preprint. Discussion started: 27 July 2026

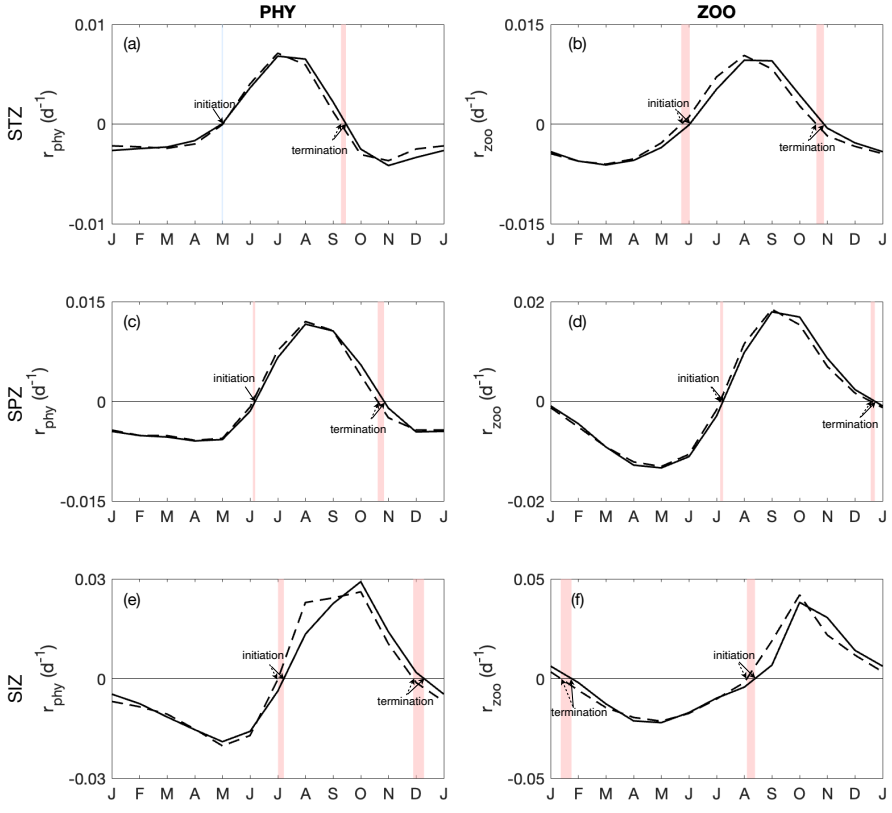

Figure C3. Present (2000s) and future (2090s) seasonality of phytoplankton (phy, a,c,e) and zooplankton (zoo, b,d,f) biomass accumulation rate (as $r_{\mathrm{bio}} = \frac{1}{\mathrm{bio}} \frac{\mathrm{d\,bio}}{\mathrm{d}t}$, following Behrenfeld et al. 2017 and Yamaguchi et al. 2022) in the STZ (a, b), SPZ (c, d), and SIZ (e, f). Red- and blue-shaded bars indicate advanced and delayed shifts in bloom initiation and termination over the century, respectively.

https://doi.org/10.5194/egusphere-2026-3722
Preprint. Discussion started: 27 July 2026

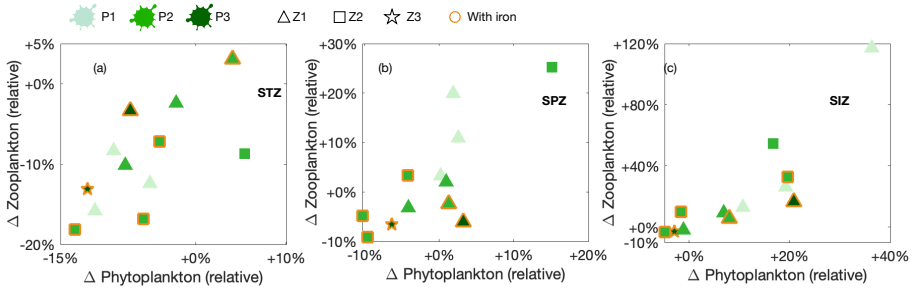

Figure C4. Individual model projections of the relative changes of integrated phytoplankton (phy, horizontal axis) and zooplankton biomass (zoo, vertical axis) in the subtropical zone (STZ, a), the subpolar zone (SPZ, b), and the seasonal ice zone (SIZ, c) over the 21st century, illustrating that there is no systematic effect of biogeochemical model complexity on the projections. The color of the markers indicates the number of phytoplankton groups included in the model, with light green, green, and dark green representing one, two, and three phytoplankton groups, respectively. The shape of the markers indicates the number of zooplankton groups included in the model, with triangle, square, and star representing one, two, and three zooplankton groups, respectively. Markers with orange edges indicate that the model explicitly includes iron limitation.

https://doi.org/10.5194/egusphere-2026-3722
Preprint. Discussion started: 27 July 2026

Author contributions. TX designed the study. TX conducted the analysis with support from LA, MP and IF. TX wrote the first draft of the manuscript and produced all figures and tables. All authors discussed the results and contributed to the final writing of the manuscript.

Competing interests. The authors declare that they have no conflict of interest.

Acknowledgements. LA was supported by NASA Carbon Monitoring System (80NSSC23K1231, Principal Investigator: LA). We acknowledge the World Climate Research Programme for coordinating and providing the CMIP6 data and we thank Chia-Te Chien for sharing FOCI data, which was essential for this study. We express our sincere appreciation to Andreas Oschlies and Michael Behrenfeld for invaluable discussions and constructive feedback and to Niels Mahrt and Haichao Guo for comments that helped to clarify the manuscript and figures.

https://doi.org/10.5194/egusphere-2026-3722
Preprint. Discussion started: 27 July 2026

References

Archibald, K. M., Dutkiewicz, S., Laufkötter, C., and Moeller, H. V.: Thermal responses in global marine planktonic food webs are mediated by temperature effects on metabolism, Journal of Geophysical Research: Oceans, 127, e2022JC018 932, https://doi.org/10.1029/2022JC018932, 2022.

Arteaga, L. A., Boss, E., Behrenfeld, M. J., Westberry, T. K., and Sarmiento, J. L.: Seasonal modulation of phytoplankton biomass in the Southern Ocean, Nature Communications, 11, 1–10, https://doi.org/10.1038/s41467-020-19157-2, 2020.

Asch, R. G., Stock, C. A., and Sarmiento, J. L.: Climate change impacts on mismatches between phytoplankton blooms and fish spawning phenology, Global Change Biology, 25, 2544–2559, https://doi.org/10.1111/gcb.14650, 2019.

Atkinson, A., Rossberg, A. G., Gaedke, U., Sprules, G., Heneghan, R. F., Batziakas, S., Grigoratou, M., Fileman, E., Schmidt, K., and Frangoulis, C.: Steeper size spectra with decreasing phytoplankton biomass indicate strong trophic amplification and future fish declines, Nature Communications, 15, 381, https://doi.org/10.1038/s41467-023-44406-5, 2024.

Behrenfeld, M. J.: Abandoning Sverdrup's critical depth hypothesis on phytoplankton blooms, Ecology, 91, 977–989, https://doi.org/10.1890/09-1207.1, 2010.

Behrenfeld, M. J., Hu, Y., O'Malley, R. T., Boss, E. S., Hostetler, C. A., Siegel, D. A., Sarmiento, J. L., Schulien, J., Hair, J. W., Lu, X., and Scarino, A. J.: Annual boom–bust cycles of polar phytoplankton biomass revealed by space-based lidar, Nature Geoscience, 10, 118–122, https://doi.org/10.1038/NGEO2861, 2017.

Boucher, O., Servonnat, J., Albright, A. L., Aumont, O., Balkanski, Y., Bastrikov, V., Bekki, S., Bonnet, R., Bony, S., Bopp, L., and Vuichard, N.: Presentation and evaluation of the IPSL-CM6A-LR climate model, Journal of Advances in Modeling Earth Systems, 12, e2019MS002 010, https://doi.org/10.1029/2019MS002010, 2020.

Bowman, D. M., Kolden, C. A., Abatzoglou, J. T., Johnston, F. H., van der Werf, G. R., and Flannigan, M.: Vegetation fires in the Anthropocene, Nature Reviews Earth & Environment, 1, 500–515, https://doi.org/10.1038/s43017-020-0085-3, 2020.

Boyd, P. W., Crossley, A., DiTullio, G., Griffiths, F., Hutchins, D., Queguiner, B., Sedwick, P. N., and Trull, T.: Control of phytoplankton growth by iron supply and irradiance in the subantarctic Southern Ocean: Experimental results from the SAZ Project, Journal of Geophysical Research: Oceans, 106, 31 573–31 583, https://doi.org/10.1029/2000JC000348, 2001.

Cabré, A., Marinov, I., and Leung, S.: Consistent global responses of marine ecosystems to future climate change across the IPCC AR5 earth system models, Climate Dynamics, 45, 1253–1280, https://doi.org/10.1007/s00382-014-2374-3, 2015.

Chien, C.-T., Durgadoo, J. V., Ehlert, D., Frenger, I., Keller, D. P., Koeve, W., Kriest, I., Landolfi, A., Patara, L., Wahl, S., and Oschlies, A.: FOCI-MOPS v1–integration of marine biogeochemistry within the Flexible Ocean and Climate Infrastructure version 1 (FOCI 1) Earth system model, Geoscientific Model Development, 15, 5987–6024, https://doi.org/10.5194/gmd-15-5987-2022, 2022.

Christian, J. R., Denman, K. L., Hayashida, H., Holdsworth, A. M., Lee, W. G., Riche, O. G., Shao, A. E., Steiner, N., and Swart, N. C.: Ocean biogeochemistry in the Canadian Earth system model version 5.0. 3: CanESM5 and CanESM5-CanOE, Geoscientific Model Development, 15, 4393–4424, https://doi.org/10.5194/gmd-15-4393-2022, 2022.

Chust, G., Allen, J. I., Bopp, L., Schrum, C., Holt, J., Tsiaras, K., Zavatarelli, M., Chifflet, M., Cannaby, H., Dadou, I., and Irigoien, X.: Biomass changes and trophic amplification of plankton in a warmer ocean, Global Change Biology, 20, 2124–2139, https://doi.org/10.1111/gcb.12562, 2014.

Cushing, D.: Marine ecology and fisheries, vol. 292, Cambridge University Press, 1975.

https://doi.org/10.5194/egusphere-2026-3722
Preprint. Discussion started: 27 July 2026

Danabasoglu, G., Lamarque, J.-F., Bacmeister, J., Bailey, D., DuVivier, A., Edwards, J., Emmons, L., Fasullo, J., Garcia, R., Gettelman, A., and Strand, W.: The community earth system model version 2 (CESM2), Journal of Advances in Modeling Earth Systems, 12, e2019MS001 916, https://doi.org/10.1029/2019MS001916, 2020.

de Boyer Montégut, C., Madec, G., Fischer, A. S., Lazar, A., and Iudicone, D.: Mixed layer depth over the global ocean: An examination of profile data and a profile-based climatology, Journal of Geophysical Research: Oceans, 109, https://doi.org/10.1029/2004JC002378, 2004.

Deppeler, S. L. and Davidson, A. T.: Southern Ocean phytoplankton in a changing climate, Frontiers in Marine Science, 4, 40, https://doi.org/10.3389/fmars.2017.00040, 2017.

Doney, S. C.: Plankton in a warmer world, Nature, 444, 695–696, https://doi.org/10.1038/444695a, 2006.

Dunne, J., Horowitz, L., Adcroft, A., Ginoux, P., Held, I., John, J., Krasting, J., Malyshev, S., Naik, V., Paulot, F., and Zhao, M.: The GFDL Earth System Model version 4.1 (GFDL-ESM 4.1): Overall coupled model description and simulation characteristics, Journal of Advances in Modeling Earth Systems, 12, e2019MS002 015, https://doi.org/10.1029/2019MS002015, 2020.

Edwards, M. and Richardson, A. J.: Impact of climate change on marine pelagic phenology and trophic mismatch, Nature, 430, 881–884, https://doi.org/10.1038/nature02808, 2004.

Frenzel, H., Sharp, J., Fassbender, A., and Buzby, N.: OneArgo-Mat: A MATLAB toolbox for accessing and visualizing Argo data., https://doi.org/10.5281/zenodo.6588041, 2022.

Gotceitas, V., Puvanendran, V., Leader, L. L., and Brown, J. A.: An experimental investigation of the 'match/mismatch' hypothesis using larval Atlantic cod, Marine Ecology Progress Series, 130, 29–37, https://doi.org/10.3354/meps130029, 1996.

Graff, J. R., Westberry, T. K., Milligan, A. J., Brown, M. B., Dall'Olmo, G., van Dongen-Vogels, V., Reifel, K. M., and Behrenfeld, M. J.: Analytical phytoplankton carbon measurements spanning diverse ecosystems, Deep Sea Research Part I: Oceanographic Research Papers, 102, 16–25, https://doi.org/10.1016/j.dsr.2015.04.006, 2015.

Haëntjens, N., Boss, E., and Talley, L. D.: Revisiting Ocean Color algorithms for chlorophyll a and particulate organic carbon in the Southern Ocean using biogeochemical floats, Journal of Geophysical Research: Oceans, 122, 6583–6593, https://doi.org/10.1002/2017JC012844, 2017.

Hamilton, D. S., Moore, J. K., Arneth, A., Bond, T. C., Carslaw, K. S., Hantson, S., Ito, A., Kaplan, J. O., Lindsay, K., Nieradzik, L., and Mahowald, N. M.: Impact of changes to the atmospheric soluble iron deposition flux on ocean biogeochemical cycles in the Anthropocene, Global Biogeochemical Cycles, 34, e2019GB006 448, https://doi.org/10.1029/2019GB006448, 2020.

Hiscock, M. R., Marra, J., Smith Jr, W. O., Goericke, R., Measures, C., Vink, S., Olson, R. J., Sosik, H. M., and Barber, R. T.: Primary productivity and its regulation in the Pacific Sector of the Southern Ocean, Deep Sea Research Part II: Topical Studies in Oceanography, 50, 533–558, https://doi.org/10.1016/S0967-0645(02)00583-0, 2003.

Holte, J., Talley, L. D., Gilson, J., and Roemmich, D.: An Argo mixed layer climatology and database, Geophysical Research Letters, 44, 5618–5626, https://doi.org/10.1002/2017GL073426, 2017.

Kwiatkowski, L., Aumont, O., and Bopp, L.: Consistent trophic amplification of marine biomass declines under climate change, Global Change Biology, 25, 218–229, https://doi.org/10.1111/gcb.14468, 2019.

Kwiatkowski, L., Torres, O., Bopp, L., Aumont, O., Chamberlain, M., Christian, J. R., Dunne, J. P., Gehlen, M., Ilyina, T., John, J. G., and Ziehn, T.: Twenty-first century ocean warming, acidification, deoxygenation, and upper-ocean nutrient and primary production decline from CMIP6 model projections, Biogeosciences, 17, 3439–3470, https://doi.org/10.5194/bg-17-3439-2020, 2020.

https://doi.org/10.5194/egusphere-2026-3722
Preprint. Discussion started: 27 July 2026

Le Grix, N. and Tagliabue, A.: Sources of uncertainty in ocean net primary productivity projections under climate change, Geophysical Research Letters, 53, e2025GL119 652, https://doi.org/10.1029/2025GL119652, 2026.

Le Quéré, C., Buitenhuis, E. T., Moriarty, R., Alvain, S., Aumont, O., Bopp, L., Chollet, S., Enright, C., Franklin, D. J., Geider, R. J., et al.: Role of zooplankton dynamics for Southern Ocean phytoplankton biomass and global biogeochemical cycles, Biogeosciences, 13, 4111–4133, https://doi.org/10.5194/bg-13-4111-2016, 2016.

Leung, S., Cabré, A., and Marinov, I.: A latitudinally banded phytoplankton response to 21st century climate change in the Southern Ocean across the CMIP5 model suite, Biogeosciences, 12, 5715–5734, https://doi.org/10.5194/bg-12-5715-2015, 2015.

Liniger, G., Sharp, J. D., Takeshita, Y., and Johnson, K. S.: Two decades of increase in Southern Ocean net community production revealed by BGC-Argo floats, Global Biogeochemical Cycles, 39, e2024GB008 371, https://doi.org/10.1029/2024GB008371, 2025.

Lotze, H. K., Tittensor, D. P., Bryndum-Buchholz, A., Eddy, T. D., Cheung, W. W., Galbraith, E. D., Barange, M., Barrier, N., Bianchi, D., Blanchard, J. L., et al.: Global ensemble projections reveal trophic amplification of ocean biomass declines with climate change, Proceedings of the National Academy of Sciences, 116, 12 907–12 912, https://doi.org/10.1073/pnas.1900194116, 2019.

Marinov, I., Doney, S., and Lima, I.: Response of ocean phytoplankton community structure to climate change over the 21st century: partitioning the effects of nutrients, temperature and light, Biogeosciences, 7, 3941–3959, https://doi.org/10.5194/bg-7-3941-2010, 2010.

McCauley, D. J., Gellner, G., Martinez, N. D., Williams, R. J., Sandin, S. A., Micheli, F., Mumby, P. J., and McCann, K. S.: On the prevalence and dynamics of inverted trophic pyramids and otherwise top-heavy communities, Ecology Letters, 21, 439–454, https://doi.org/10.1111/ele.12900, 2018.

Moore, C., Mills, M., Arrigo, K., Berman-Frank, I., Bopp, L., Boyd, P., Galbraith, E., Geider, R., Guieu, C., Jaccard, S., and Ulloa, O.: Processes and patterns of oceanic nutrient limitation, Nature Geoscience, 6, 701–710, https://doi.org/10.1038/ngeo1765, 2013.

Müller, W. A., Jungclaus, J. H., Mauritsen, T., Baehr, J., Bittner, M., Budich, R., Bunzel, F., Esch, M., Ghosh, R., Haak, H., and Marotzke, J.: A higher-resolution version of the max planck institute earth system model (MPI-ESM1. 2-HR), Journal of Advances in Modeling Earth Systems, 10, 1383–1413, https://doi.org/10.1029/2017MS001217, 2018.

Nissen, C., Gruber, N., Münnich, M., and Vogt, M.: Southern Ocean phytoplankton community structure as a gatekeeper for global nutrient biogeochemistry, Global Biogeochemical Cycles, 35, e2021GB006 991, https://doi.org/10.1029/2021GB006991, 2021.

O'Brien, T. D.: COPEPOD, a global plankton database: A review of the 2007 database contents and new quality control methodology, URL: https://repository.library.noaa.gov/view/noaa/5039, 2007.

Pahlow, M., Chien, C.-T., Arteaga, L. A., and Oschlies, A.: Optimality-based non-Redfield plankton–ecosystem model (OPEM v1. 1) in UVic-ESCM 2.9–Part 1: Implementation and model behaviour, Geoscientific Model Development, 13, 4663–4690, https://doi.org/10.5194/gmd-13-4663-2020, 2020.

Ratnarajah, L., Abu-Alhaija, R., Atkinson, A., Batten, S., Bax, N. J., Bernard, K. S., Canonico, G., Cornils, A., Everett, J. D., Grigoratou, M., and Yebra, L.: Monitoring and modelling marine zooplankton in a changing climate, Nature Communications, 14, 564, https://doi.org/10.1038/s41467-023-36241-5, 2023.

Rohr, T., Richardson, A. J., Lenton, A., Chamberlain, M. A., and Shadwick, E. H.: Zooplankton grazing is the largest source of uncertainty for marine carbon cycling in CMIP6 models, Communications Earth & Environment, 4, 212, https://doi.org/10.1038/s43247-023-00871-w, 2023.

Ryan-Keogh, T. J., Thomalla, S. J., Monteiro, P. M., and Tagliabue, A.: Multidecadal trend of increasing iron stress in Southern Ocean phytoplankton, Science, 379, 834–840, https://doi.org/10.1126/science.abl5237, 2023.

https://doi.org/10.5194/egusphere-2026-3722
Preprint. Discussion started: 27 July 2026

Sallée, J.-B., Pellichero, V., Akhoudas, C., Pauthenet, E., Vignes, L., Schmidtko, S., Garabato, A. N., Sutherland, P., and Kuusela, M.: Summertime increases in upper-ocean stratification and mixed-layer depth, Nature, 591, 592–598, https://doi.org/10.1038/s41586-021-03303-x, 2021.

Sarmiento, J. L., Gruber, N., Brzezinski, M., and Dunne, J.: High-latitude controls of thermocline nutrients and low latitude biological productivity, Nature, 427, 56–60, https://doi.org/10.1038/nature02127, 2004a.

Sarmiento, J. L., Slater, R., Barber, R., Bopp, L., Doney, S., Hirst, A., Kleypas, J., Matear, R., Mikolajewicz, U., Monfray, P., and Stouffer, R.: Response of ocean ecosystems to climate warming, Global Biogeochemical Cycles, 18, https://doi.org/10.1029/2003GB002134, 2004b.

Séférian, R., Nabat, P., Michou, M., Saint-Martin, D., Voldoire, A., Colin, J., Decharme, B., Delire, C., Berthet, S., Chevallier, M., S., S., and Madec, G.: Evaluation of CNRM earth system model, CNRM-ESM2-1: Role of earth system processes in present-day and future climate, Journal of Advances in Modeling Earth Systems, 11, 4182–4227, https://doi.org/10.1029/2019MS001791, 2019.

Séférian, R., Berthet, S., Yool, A., Palmieri, J., Bopp, L., Tagliabue, A., Kwiatkowski, L., Aumont, O., Christian, J., Dunne, J., and Yamamoto, A.: Tracking improvement in simulated marine biogeochemistry between CMIP5 and CMIP6, Current Climate Change Reports, 6, 95–119, https://doi.org/10.1007/s40641-020-00160-0, 2020.

Sellar, A. A., Jones, C. G., Mulcahy, J. P., Tang, Y., Yool, A., Wiltshire, A., O'connor, F. M., Stringer, M., Hill, R., Palmieri, J., and Zerroukat, M.: UKESM1: Description and evaluation of the UK Earth System Model, Journal of Advances in Modeling Earth Systems, 11, 4513–4558, https://doi.org/10.1029/2019MS001739, 2019.

Shurin, J. B., Gruner, D. S., and Hillebrand, H.: All wet or dried up? Real differences between aquatic and terrestrial food webs, Proceedings of the Royal Society B: Biological Sciences, 273, 1–9, https://doi.org/10. 1098/rspb.2005.3377, 2006.

Steinacher, M., Joos, F., Frölicher, T., Bopp, L., Cadule, P., Cocco, V., Doney, S., Gehlen, M., Lindsay, K., Moore, J., and Segschneider, J.: Projected 21st century decrease in marine productivity: a multi-model analysis, Biogeosciences, 7, 979–1005, https://doi.org/10.5194/bg-7-979-2010, 2010.

Stock, C., Dunne, J., and John, J.: Drivers of trophic amplification of ocean productivity trends in a changing climate, Biogeosciences, 11, 7125–7135, https://doi.org/10.5194/bg-11-7125-2014, 2014.

Swart, N. C., Cole, J. N., Kharin, V. V., Lazare, M., Scinocca, J. F., Gillett, N. P., Anstey, J., Arora, V., Christian, J. R., Hanna, S., and Winter, B.: The Canadian earth system model version 5 (CanESM5. 0.3), Geoscientific Model Development, 12, 4823–4873, https://doi.org/10.5194/gmd-12-4823-2019, 2019.

Tagliabue, A., Aumont, O., DeAth, R., Dunne, J. P., Dutkiewicz, S., Galbraith, E., Misumi, K., Moore, J. K., Ridgwell, A., Sherman, E., and Yool, A.: How well do global ocean biogeochemistry models simulate dissolved iron distributions?, Global Biogeochemical Cycles, 30, 149–174, https://doi.org/10.1002/2015GB005289, 2016.

Thomalla, S., Fauchereau, N., Swart, S., and Monteiro, P.: Regional scale characteristics of the seasonal cycle of chlorophyll in the Southern Ocean, Biogeosciences, 8, 2849–2866, https://doi.org/10.5194/bg-8-2849-2011, 2011.

Thomalla, S., Nicholson, S.-A., Ryan-Keogh, T. J., and Smith, M. E.: Widespread changes in Southern Ocean phytoplankton blooms linked to climate drivers, Nature Climate Change, pp. 1–10, https://doi.org/10.1038/s41558-023-01768-4, 2023b.

Tjiputra, J. F., Schwinger, J., Bentsen, M., Morée, A. L., Gao, S., Bethke, I., Heinze, C., Goris, N., Gupta, A., He, Y.-C., and Schulz, M.: Ocean biogeochemistry in the Norwegian Earth System Model version 2 (NorESM2), Geoscientific Model Development, 13, 2393–2431, https://doi.org/10.5194/gmd-13-2393-2020, 2020.

https://doi.org/10.5194/egusphere-2026-3722
Preprint. Discussion started: 27 July 2026

Tsujino, H., Nakano, H., Sakamoto, K., Urakawa, S., Hirabara, M., Ishizaki, H., and Yamanaka, G.: Reference manual for the Meteorological Research Institute Community Ocean Model version 4 (MRI. COMv4), Technical Reports of the Meteorological Research Institute, 80, 306, 2017.

Vives, C. R., Schallenberg, C., Strutton, P. G., and Boyd, P. W.: Biogeochemical-Argo floats show that chlorophyll increases before carbon in the high-latitude Southern Ocean spring bloom, Limnology and Oceanography Letters, 9, 172–182, https://doi.org/10.1002/lol2.10322, 2024.

Weis, J., Chase, Z., Schallenberg, C., Strutton, P. G., Bowie, A. R., and Fiddes, S. L.: One-third of Southern Ocean productivity is supported by dust deposition, Nature, 629, 603–608, https://doi.org/10.1038/s41586-024-07366-4, 2024.

Westwood, K. J., Griffiths, F. B., Meiners, K. M., and Williams, G. D.: Primary productivity off the Antarctic coast from 30–80 E; BROKE-West survey, 2006, Deep Sea Research Part II: Topical Studies in Oceanography, 57, 794–814, https://doi.org/10.1016/j.dsr2.2008.08.020, 2010.

Woodward, S., Roberts, D., and Betts, R.: A simulation of the effect of climate change–induced desertification on mineral dust aerosol, Geophysical Research Letters, 32, https://doi.org/10.1029/2005GL023482, 2005.

Xue, T. and Hill, M.: Phenological mismatch contributes to anchoveta landings collapse under El Niño and climate change in the Peruvian upwelling system, ICES Journal of Marine Science, 82, fsaf214, https://doi.org/10.1093/icesjms/fsaf214, 2025.

Xue, T., Frenger, I., Oschlies, A., Stock, C. A., Koeve, W., John, J. G., and Prowe, A. E.: Mixed layer depth promotes trophic amplification on a seasonal scale, Geophysical Research Letters, 49, e2022GL098 720, https://doi.org/10.1029/2022GL098720, 2022a.

Xue, T., Frenger, I., Prowe, A., José, Y. S., and Oschlies, A.: Mixed layer depth dominates over upwelling in regulating the seasonality of ecosystem functioning in the Peruvian upwelling system, Biogeosciences, 19, 455–475, https://doi.org/10.5194/bg-19-455-2022, 2022b.

Xue, T., Frenger, I., Hauschildt, J., and Oschlies, A.: Mechanisms regulating trophic transfer in the Humboldt Upwelling System differ across time scales, Environmental Research Letters, 19, 114 014, https://doi.org/10.1088/1748-9326/ad78ec, 2024a.

Xue, T., Terhaar, J., Prowe, A. F., Frölicher, T. L., Oschlies, A., and Frenger, I.: Southern Ocean phytoplankton under climate change: a shifting balance of bottom-up and top-down control, Biogeosciences, 21, 2473–2491, https://doi.org/10.5194/bg-21-2473-2024, 2024b.

Yamaguchi, R., Rodgers, K. B., Timmermann, A., Stein, K., Schlunegger, S., Bianchi, D., Dunne, J. P., and Slater, R. D.: Trophic level decoupling drives future changes in phytoplankton bloom phenology, Nature Climate Change, 12, 469–476, https://doi.org/10.1038/s41558-022-01353-1, 2022.

Yang, G., Atkinson, A., Pakhomov, E. A., Hill, S. L., and Racault, M.-F.: Massive circumpolar biomass of Southern Ocean zooplankton: Implications for food web structure, carbon export, and marine spatial planning, Limnology and Oceanography, 67, 2516–2530, https://doi.org/10.1002/lno.12219, 2022.